Journal Pre-proofs

Formation of stable nanoemulsions by ultrasound-assisted two-step emulsification process for topical drug delivery: effect of oil phase composition and surfactant concentration and loratadine as ripening inhibitor

Omar Sarheed, Douha Shouqair, KVRNS Ramesh, Taha Khaleel, Muhammad Amin, Joshua Boateng, Markus Drechsler

PII: S0378-5173(19)30997-4
DOI: https://doi.org/10.1016/j.ijpharm.2019.118952
Reference: IJP 118952

To appear in: *International Journal of Pharmaceutics*

Received Date: 1 September 2019
Revised Date: 14 November 2019
Accepted Date: 11 December 2019

Please cite this article as: O. Sarheed, D. Shouqair, K. Ramesh, T. Khaleel, M. Amin, J. Boateng, M. Drechsler, Formation of stable nanoemulsions by ultrasound-assisted two-step emulsification process for topical drug delivery: effect of oil phase composition and surfactant concentration and loratadine as ripening inhibitor, *International Journal of Pharmaceutics* (2019), doi: https://doi.org/10.1016/j.ijpharm.2019.118952

Formation of stable nanoemulsions by ultrasound-assisted two-step emulsification process for topical drug delivery: effect of oil phase composition and surfactant concentration and loratadine as ripening inhibitor

Omar Sarheed[1*], Douha Shouqair[1], KVRNS Ramesh[1], Taha Khaleel[1], Muhammad Amin[2], Joshua Boateng[2] and Markus Drechsler[3]

[1]RAK College of Pharmaceutical Sciences, RAK Medical and Health Sciences University, Ras AlKhaimah, United Arab Emirates.

[2] School of Science, Faculty of Engineering and Science, University of Greenwich, UK.

[3] Bavarian Polymer Institute, KeyLab "Electron and Optical Microscopy", University of Bayreuth, Germany.

* To whom correspondence should be addressed:

Dr. Omar Sarheed (sarheed@rakmhsu.ac.ae; sarheed78@gmail.com)

Abstract

Nanoemulsions are very interesting systems as they offer capacity to encapsulate both hydrophilic and lipophilic molecules in a single particle, as well as the controlled release of chemical moieties initially entrapped in the internal droplets. In this study, we propose a new two-step modified ultrasound-assisted phase inversion approaches-phase inversion temperature (PIT) and self-emulsification, to prepare stable o/w nanoemulsions from a fully water-dilutable microemulsion template for the transdermal delivery of loratadine (a hydrophobe and as Ostwald ripening inhibitor). Firstly, the primary water-in-oil microemulsion concentrate (w/o) was formed using loratadine in the oil phase (oleic acid or coconut oil) and Tween 80 in the aqueous phase and by adjusting the PIT around 85 °C followed by stepwise dilution with water at 25 °C to initiate the formation the nanoemulsions (o/w). To assure the long-term stability, a brief application of low frequency ultrasound was employed. Combining the two low energy methods resulted in nanoemulsions prepared by mixing constant surfactant/oil ratios above the PIT with varying water volume fraction (self-emulsification) during the PIT by stepwise dilution. The kinetic stability was evaluated by measuring the droplet size with time by dynamic light scattering (DLS). The droplet size ranged 15-43 nm and did not exceed 100 nm over the period of over the 6 months indicating the system had high kinetic stability. Cryo-TEM showed the nanoemulsions droplets were monodispersed and approaching micellar structure and scale. All nanoemulsions had loratadine crystals formed within 20 days after preparation, which inclined to sediment during storage. Nanoemulsions improved the in vitro permeation of loratadine through porcine skin up to 20 times compared to the saturated solution.

Keywords:

Nanoemulsion; Phase inversion temperature (PIT) method; Nonionic; Transdermal drug delivery; Ultrasound; Ostwald ripening; Coalescence.

Introduction

Microemulsions and nanoemulsions attract interest as delivery systems for different moieties. They demonstrate droplet radii up to 500 nm with optimal system stability when the droplet size is less than 100 nm (McClements, 2012).

A major drawback with microemulsions is the high surfactant and/or co-surfactant composition, which may make them potentially toxic upon administration. Therefore nanoemulsions can be an alternative as they share most of the good qualities of microemulsions- (apart from being thermodynamically unstables) - and can be formed at surfactant concentrations lower than required in microemulsions.

One important aspect in the fabrication of nanoemulsions is the application of external energy to break the kinetic energy barrier of the immiscible components (oil and water). The energy applied should exceed the positive free energy of oil and water while in contact and the use of low frequency ultrasound (20 kHz) is justified by its ability to generate the required intense disruptive forces exceeding the forces that hold the droplets into spherical shape (Leong et al., 2009). The particle size of nanoemulsions tends to decrease as the ultrasonic intensity increases and tend to be more stable and less polydispersed with the use of ultrasound.

One major drawback of high-energy methods is that less than 0.1% of the mechanical energy is utilized for the emulsification (Tadros et al., 2004). Thus, the use of low-energy is an alternative, which employs the intrinsic physicochemical properties of the emulsion components.

Phase inversion temperature (PIT) was firstly reported by Shinoda and Saito (1969) which depends on the surfactant's solubility changing from aqueous to oily phase with temperature and involves the mixing of oil, water and nonionic surfactant (such as polyethoxylated surfactants) at room

temperature with gentle stirring. A two-step process for the formation of finely dispersed emulsions for cosmetic use, with long-term stability, was described by (Wadle et al., 1993).

One key aspect in the fabrication of nanoemulsions by PIT method is the utilization of high surfactant-to-oil ratio (SOR) to prepare the microemulsion base which will be used later to form the nanoemulsion by cooling and dilution at room temperature. The stability of nanoemulsions is a major challenge and are thermodynamically unstable even closer to the demixing line of microemulsions but kinetically stable systems (Delmas et al., 2011b). Factors such as the control of particle size distribution, the incorporation of stabilizers such as Ostwald ripening retarding agent or by using a suitable emulsifier type to prevent coalescence are employed to improve kinetic stability.

It is reported that supersaturated vehicles can enhance drug absorption by the skin with high thermodynamic activity (Kemken et al., 1992). In this regard, microemulsions present a vehicle with decreasing water solubility for lipophilic molecules as the amount of water increases, which is the case during the preparation of nanoemulsion by the dilution method. Secondly, the drug incorporated within primary microemulsion can undergo in vitro crystallization very slowly after the preparation, which could take up to 10-14 days with no crystal observed within the first 2-3 days after formation of the supersaturated systems (Kemken et al., 1992).

The use of ultrasound-assisted phase inversion method will offer industrial benefits such as reduction in the amount of surfactants, easy manufacturing and processing of low-viscosity oil-in-water nanoemulsions and short application of ultrasound that will produce a stable nanoemulsion. This will save the costs from applying high-energy ultrasound alone and will be more environmentally friendly and sustainable.

The aim of this work was to develop and characterize a stable nanoemulsion containing a saturated concentration of loratadine by ultrasound-assisted phase inversion method for transdermal drug delivery and investigate the effect of oil phase composition and surfactant concentration on the skin permeation of the drug. Loratadine was employed as a model 'very lipophilic' drug and to act as an Ostwald ripening inhibitor, which is reported for the first time. It is also the first time a nanoemulsion prepared by ultrasound-assisted two-step phase inversion and cooling-stepwise dilution method, loaded with near saturation concentration (C_{sat}) of oil phase, with a drug molecule from w/o microemulsion for transdermal drug delivery.

2. Materials and methods

2.1 Materials

Loratadine was kindly donated by Gulf Pharmaceutical Industries (Julphar, UAE). Oleic acid and orthophosphoric acid were purchased from Avonchem limited (UK). Coconut oil (chemically pure grade) was provided by Labchem products (USA). Tween 80, Tween 60, Span 60 and potassium phosphate monobasic were obtained from Sigma Aldrich Co. (USA) and of chemically pure grade. Tween 80 was of POE (20). Acetonitrile and methanol of HPLC grade were purchased from VWR BDH Prolabo Chemicals (UK). Water for HPLC was provided by Fisher Scientific (UK). Cellulose acetate dialysis membrane was obtained from HiMedia Laboratories Pvt. Ltd. (India). Polydimethylsiloxane membrane (PDMS) was purchased from Samco (UK). All other solvents and reagents used were of analytical grade.

2.2 Determination of loratadine solubility in lipids

In preliminary experiments, it was found that a system composed of lipids other than oleic acid and coconut oil formed cloudy and unstable emulsions and they were discontinued from further investigations. In addition to that oleic acid and coconut oil were chosen due to their safety profiles, potential penetration enhancing activity and their use in cosmetic formulations (Viljoen et al., 2015). These oils are relatively inexpensive and economically more readily available.

To determine the solubility of loratadine in lipids, we adopted the method reported by Patel and co-workers (Patel et al., 2012). 50 mg of loratadine was transferred into a mortar maintained at temperature of 10 °C above the melting point of the lipid (~85 °C), and the lipid (oleic acid and coconut oil) was added gradually in increments of 50 mg and mixed, till loratadine was completely dissolved. The amount of lipid required to solubilize loratadine was noted by visualizing the disappearance of drug crystals and formation of a transparent homogeneous system and this was recorded (Cirri et al., 2018).

2.3 Loratadine partitioning into lipids

Partitioning behavior of loratadine between water and the lipids (oleic acid and coconut oil) was tested following the method reported by Venkateswarlu and Manjunath (2004) with slight modifications to mimic the experimental conditions needed for nanoemulsion production. This was performed by adding a known amount (10 mg) of loratadine to a mixture of equal volumes of hot distilled water and molten lipid. The mixture was shaken at 120 rpm for 2-4 hours in a hot water bath maintained at 10 °C above the lipid melting point (~85 °C) as previously reported by Joshi and Patravale, (2008) and Wong et al. (2004). Then the aqueous phase was separated after cooling by ultra-centrifugation at 25000 rpm for 20 minutes. The drug content in the supernatant

was determined by HPLC-UV at 247 nm and the percentage of partitioning was calculated using the following formula:

$$(\%)Partition = \frac{Amount\ of\ drug\ added - Amount\ of\ drug\ in\ supernatant}{Amount\ of\ drug\ added}$$

2.4 Formation of nanoemulsions

A combination of low-energy (PIT) and high-energy (ultrasonication) techniques were employed to form nanoemulsions. A number of surfactants (Tween 80, Tween 60 and Span 60) were screened with different lipids (bees wax, carnauba wax, cetyl alcohol, coconut oil and oleic acid) in preliminary studies. Only coconut oil, oleic acid and Tween 80 were selected to proceed with further studies and three different ratios of lipid to surfactant 1:5, 1:7 and 1:10 were employed. The order of mixing was done by two methods named as 'Method 1' and 'Method 2'.

2.4.1 Method 1

In Method 1, 75 mg of loratadine was dissolved in appropriate amount of oil (coconut oil and oleic acid) at 85 °C. The amount of oil added was based on loratadine solubility in the oil. Aqueous solution of Tween 80 was prepared separately and heated to the same temperature as the oil phase, then added drop wise to the lipid phase under homogenization with an Ultra-Turrax® homogenizer (IKA T25, Germany) at 14000 rpm for 5 min, to obtain a homogenous dispersion. Throughout the homogenization, the temperature was adjusted to 10 °C above the PIT. The PIT was determined using electrical conductivity measurements with rise in temperature and the cloud points in water and oil were visually defined. The resultant emulsion was subjected to sonication using a probe sonicator (300 V/T ultrasonic homogenizer, BioLogics Inc, USA) at a frequency of 20 kHz and power of 50% for 5 min with temperature maintained 10 °C above the PIT. Finally, the emulsion was rapidly diluted with water at room temperature under mild stirring using paddle stirrer at 500

rpm resulting in rapid formation of the nanoemulsions. The final ratio of nanoemulsion to aqueous media was 1:5 and the final water concentration was kept constant at 96-98%.

2.4.2 Method 2

The preparation in Method 2, was the same as in Method 1, however, the resultant emulsion was added drop wise to distilled water at room temperature using Ultra-Turrax® at 14000 rpm for 5 min, to produce a nanoemulsion to aqueous media ratio of 1:5. Then the nanoemulsion was allowed to settle, and sonicated at room temperature using probe sonicator (300 V/T ultrasonic homogenizer, BioLogics Inc, USA) at a frequency of 20 kHz and power of 70% for 5 min. The final water concentration was kept constant at 96-98%. The effect of composition parameters, including the oil-to-surfactant weight ratio (O/S) and the droplet volume fraction (φ), was explored. The nanoemulsion components are defined by the following ratios:

i. oil/surfactant weight ratio (O/S) = $100 \times w_{oil}/(w_{oil} + w_{surfactant})$

ii. droplet volume fraction (φ) = $\varphi_{oil} + \varphi_{surfactant}$.

2.4.3 Determination of cloud point

The cloud points of 0.6, 0.84 and 1.2 wt % Tween 80 ($C_{17}H_{33}$) in water were determined by measuring the turbidity variation at 660 nm, as the temperature rose from 25 to 90 °C. The experiments (n = 3) were performed on a Litesizer 500 particle analyzer (Anton Paar, Austria) equipped with a Peltier temperature-control device, and the sample was measured using 1 cm Hellma quartz cuvette.

2.4.4 Determination of PIT by turbidity measurements

Turbidity measurements were used to determine the PIT of the nanoemulsions prepared using Methods 1 and 2 above. These systems were measured using Hellma quartz cuvette and subjected to a controlled heating/cooling cycle using Litesizer 500 particle analyzer (Anton Paar, Austria) fitted out with a Peltier temperature-control device. The samples were heated from 25 to 90 °C at 5 °C / min, retained at 90 °C for 10 min, and then cooled from 90 to 25 °C at 5 °C / min. Turbidity *versus* temperature curves at 660 nm were plotted.

2.4.5 Electrical conductivity measurements

Electrical conductivity was used to determine the occurrence of phase inversion (i.e., from o/w to w/o or vice versa) during heating in the samples. A small amount of salt (7 mM NaCl) was added into the samples to increase their electrical conductivity. The samples were constantly mixed with the help of an Ultra-Turrax® homogenizer (IKA T25, Germany) during temperature-scanning electrical conductivity measurements (HANNA-HI 8733, USA). The emulsions were heated steadily using a temperature-controlled hot plate, and the conductivity was measured as a function of temperature upon the gradual addition of water.

2.5 Nanoemulsions solubilization capacity

Loratadine was added into the nanoemulsion vehicles to give a final concentration of 0.06-0.3 % (w/w), under continuous stirring at room temperature. The samples were held in tightly sealed glass vials and stored at room temperature for 48 h. Nanoemulsions with good capacity for solubilization were defined as clear and transparent liquids free of blurriness and/or precipitate.

2.6 Drug-loading and encapsulation efficiency

Triplicate samples (n = 3) of nanoemulsions were ultra-centrifuged at 25000 rpm for 30 min and the obtained supernatant was analyzed using HPLC-UV. The following equations were used in calculating for the percentage of drug loading (DL) and encapsulation efficiency (EE):

$$EE(\%) = \frac{Total\ amount\ of\ drug\ added - Amount\ of\ drug\ in\ the\ supernatant\ x100}{Total\ amount\ of\ drug\ added}$$

$$DL(\%) = \frac{Total\ drug\ added - Weight\ of\ free\ drug\ x100}{Weight\ of\ oil\ used}$$

High performance liquid chromatography (HPLC) was used to analyze loratadine. The stationary phase was Restec®, allure C18, 150 × 4.6 mm, 5µ, column (USA). The column temperature was maintained at 25 °C and the retention time was 3 min with injection volume of 20 µL. The mobile phase consisted of buffer (0.05 M monobasic potassium phosphate), acetonitrile and methanol (38:45:17 v/v) and the pH was adjusted with ortho phosphoric acid to 3.0 ± 0.2. The flow rate of the mobile phase was fixed at 1.0 mL min^{-1} and UV detection at 247 nm (Ramulu, 2011). A calibration curve was plotted from loratadine standards ranging from 2 µg/mL to 100 µg/mL (R^2 = 0.998).

2.7 Particle size, polydispersity index (PDI) and zeta potential measurements

Particles size measurements were determined using a Zetasizer Nano-ZS90 (Malvern Instruments, UK) laser diffraction instrument, using disposable sizing cuvette for size and PDI analysis. Zeta potential was measured using by measuring the surface charge using the same instrument with the help of a reusable folded capillary zeta cell, Malvern Model: DTS1070 at the Greenwich of University. The scattering angle was set at 173° and wavelength of 633 nm as required and analyses were carried out at 25 °C temperature. Samples were diluted before particle size and PDI

measurements, but zeta potential measurements were carried out without dilution. Particle size and PDI were used to evaluate the influence of SOR on nanoemulsion properties. All readings were determined in triplicates and the average values were calculated.

2.8 In vitro release studies

The effect of SOR on the loratadine release from the nanoemulsions was determined using Franz diffusion cells (V3A-02 PermeGear, USA) and to assess their release kinetics. Each cell had a surface area of 0.64 cm^2 which was filled with 1 mL of nanoemulsion and a receptor compartment volume of 5.3 mL. The receptor compartment was filled with a hydroethanolic solution (1:1) to allow drug solubilization in the media and provide sink conditions and thermodynamic balance. The receptor medium was stirred with magnetic stirrer at 600 rpm and the temperature was maintained at 37 ± 0.5 °C by the use of a thermostatic water pump (Haake SC 100, Thermo Fisher Scientific, USA). The two compartments were separated by cellulose dialysis membrane (MWCO 12-14 kDa, HiMedia Laboratories Pvt. Ltd., India) and the cellulose membrane exerts no resistance on particles moving across. The membrane was soaked overnight in distilled water prior to use, then cut to fit the surface area of Franz cell.

The donor compartment was filled with 1 mL of the formulation, and was sealed with a taut layer of Parafilm M® to minimize evaporation. The release proceeded for 24 h in which 1 mL sample of receiver solution was withdrawn at predetermined time intervals and replaced with the same volume of fresh receptor media. The obtained samples were analyzed by HPLC-UV at 247 nm. The loratadine concentration values derived for each sample was corrected for the progressive dilution occurring during the course of the experiment. The experiments were performed in triplicates (n = 3) and the average values were calculated. The obtained release profiles were

compared by applying model dependent approach using Higuchi model, zero order and first order mathematical equations

2.9 Skin preparation

Frozen pig ears were used in the study and the external surface of the ear was sectioned horizontally by surgical scalpel under laminar airflow to obtain full thickness skin. The obtained skin was visually checked for integrity, cleaned and stored frozen at -18 °C until use within one month. Few hours before the permeation study, a piece of skin was allowed to thaw to room temperature, and then cut to smaller pieces that fit the surface area of Franz cell. The skin pieces were mounted on the Franz cell and allowed to hydrate for one hour before running the study.

2.10 Pig skin permeation studies

Hydroethanolic receptor medium (1:1) was mixed and sonicated for 5 min in an ultrasonic water bath to remove air bubbles and 5.3 mL was used to fill the receiver compartment in Franz diffusion cells. The donor compartment was filled with 1 mL of nanoemulsion sample. The media was stirred at 600 rpm with magnetic stirrer and temperature was maintained at 37 ± 0.5 °C. The skin membrane was mounted on the donor compartment to separate it from the receiver compartment. Franz cells were occasionally inverted to allow the escape of any air bubbles that had formed on the skins' underside. 1 mL of the formulation was placed in the donor compartment of the Franz diffusion cell and sealed with a taut layer of Parafilm M® to minimize evaporation. The permeation studies were run for 24 h and the samples were analyzed using HPLC. Loratadine concentration values derived for each sample was corrected for the progressive dilution occurring during the course of the experiment. The experiments were performed in triplicates (n = 3) and the average

values were calculated. Amount of loratadine from the different formulations permeating the skin was compared to the permeation of saturated loratadine solution.

2.11 Cryogenic-transmission electron microscopy (cryo-TEM) Imaging

For cryo transmission electron microscopy studies, a sample droplet of 2ul was put on a lacey carbon filmed copper grid (Science Services, Muenchen, Germany resp. Quantifoil R2/2, Quantifoil Micro Tools GmbH, Jena, Germany), which was hydrophilized by air plasma glow discharge unit (30s with 50W, Solarus 950, Gatan, Munich, Germany). Subsequently, most of the liquid was removed with blotting paper in a Leica EM GP (Wetzlar, Germany) grid plunge device, leaving a thin film stretched over the lace holes in the saturated water atmosphere of the environmental chamber. The specimens were instantly shock frozen by rapid immersion into liquid ethane cooled to approximately 97K by liquid nitrogen in the temperature-controlled freezing unit of the Leica EM GP. The temperature was monitored and kept constant in the chamber during all the sample preparation steps. The specimen was inserted into a cryotransfer holder (CT3500, Gatan, Munich, Germany) and transferred to a Zeiss / LEO EM922 Omega EFTEM (Zeiss Microscopy GmbH, Jena, Germany). Examinations were carried out at temperatures around 95K. The TEM was operated at an acceleration voltage of 200kV. Zero-loss filtered images ($\Delta E = 0eV$) were taken under reduced dose conditions (100 – 1000 e/nm2). All images were registered digitally by a bottom mounted CCD camera system (Ultrascan 1000, Gatan, Munich, Germany) combined and processed with a digital imaging processing system (Digital Micrograph GMS 1.9, Gatan, Munich, Germany).

2.12 Stability studies

Formulations prepared with different lipids and surfactant ratios were stored in sealed clean glass vials at room temperature (25 °C) and at cold temperature (8 °C) for 6 months. The stored formulations were monitored and assessed periodically for particle size using Litesizer 500 (Anton Paar, Austria) and zeta potential changes, in addition to alterations in the physical appearance such as gelation, precipitation and drug crystallization. The surface coverage of oil drops by surfactant (Γ) was calculated using Langmuir isotherm model:

$$\Gamma = \Gamma_{sat} C/(k_d + C)$$

where Γ_{sat} is the saturation adsorption, C is the surfactant concentration, and k_d is the adsorption coefficient. As reported by Penfold et al. (2015) , Tween 80 (POE 20) has Γ_{sat} and k_d values of 1.4×10^{-10} mol cm^{-2} and 2.7 μM.

2.13 Statistical analysis

Quantitative data were obtained in triplicates ($n = 3$) and are reported as mean ± standard deviation. Statistical analyses were performed using Minitab version 14 software and analysis of variance (one- way ANOVA) and post hoc Tukey's test were performed. A p value < 0.05 was considered statistically significant.

3. Results and discussion

3.1 Lipids screening

Different lipids were screened for potential use in the preparation of nanoemulsions. In each experiment, different amounts of loratadine were dissolved incrementally in hot melted lipids to determine the amount of lipid required to solubilize the drug to its saturation solubility to achieve drug-enriched core nanoemulsions (Mishra et al., 2018) as shown in Table 1. Drug supersaturation

occurs during cooling of the nanoemulsion and causes precipitation of the drug before the precipitation of lipid. This results in the precipitating lipid to surround the precipitated drug, forming a membrane around incorporated drug (Mishra et al., 2018). Loratadine solubility was found to be maximum in stearic acid, followed by oleic acid, cetyl alcohol, stearyl alcohol, coconut oil, beeswax and carnuba wax. However, stearic acid, stearyl alcohol, cetyl alcohol and carnuba (data not published) failed to produce stable nanoparticles.

The results were confirmed by the preparation of loratadine standard curve in ethanol/water (1:1) and measured at 247 nm. The drug is highly lipophilic (log $K_{o/w}$ = 5.2) and it's partitioning into lipids (oleic acid and coconut oil) was above 90%.

Generally, o/w nanoemulsions are preferred for the solubilization of lipophilic molecules. It was reported that food-grade oils are not a good choice for the solubilization of large amounts of lipophilic drugs (Azeem et al., 2009). However, the amount of loratadine dissolved in oleic acid and coconut oil was 100 and 200 mg respectively. This is consistent with previous data reported by Tavares et al., (2016) and Song and Shin (2009) showed that 0.05 to 5.0% (w/w) of loratadine is preferred to penetrate the skin so as to achieve the desired therapeutic effect. In this study, nanoemulsions had loratadine concentrations from 0.06-0.3%, which are pharmaceutically acceptable.

Mechanistically, Rane and Anderson (2008) suggested that highly lipophilic molecules predominantly dissolve in the oil phase compared to surfactant and water. This has an impact on the partitioning of drug out of the oil and on the drug release.

Table 1

3.2 Preparation of nanoemulsion

Blank and drug loaded nanoemulsions were prepared by two methods which involved different order of mixing and homogenization using the lipids screened and Tween 60, Span 60 and Tween 80 at three different ratios of lipid to surfactant 1:5, 1:7 and 1:10 and the composition for the various formulations are shown in Table 2. The amount of lipids was determined by the drug solubility in the lipids (Lopes, 2014) and the solubilization capacity of a given amount of surfactant to incorporate the maximum amount of oil (Rao and McClements, 2012). High amounts of lipids beyond 10% (w/w) increases the viscosity of the dispersion and decreases the efficiency of homogenization which leads to high particle size and PDI, resulting in particles agglomeration and therefore nanoemulsion instability (Mehnert W, 2001). The total amount of oil phase including the drug (C_{Sat}) in this study was 0.3-1.5% (w/w), to assure good solubilization capacity by surfactant, small particle size and long stability as well as to ensure the formation of transparent solutions (Rao and McClements, 2012). To achieve an optimal particle size, Tween 80 was chosen and its concentration determined based on the preliminary solubilization experiments taking into consideration that the total surfactant concentration should be non-irritant and safe for transdermal application.

Table 2

3.2.1 Phase behavior of nanoemulsion

Based on the physical appearance, particle size, zeta potential and stability, formulations were optimized and further characterized. Initially, the physical appearance of the formulations were evaluated based on the visual clarity. A transparent to translucent liquid was considered as a primary indicator of smaller particle size as shown in Fig. 1.

Figure 1

Formulations prepared with Tween 60 and Span 60 were excluded due to the formation of white gel like structures. This gelation indicates limited solubilization capacity of Tween 60 and Span 60 and may be attributed to the limited mobility of the lipid which prevents the surfactant from complete coverage of the particle interface (Blanco-Prieto et al., 2015). Only formulations with Tween 80 showed good physical appearance and stability.

We characterized the phase behavior of would-be nanoemulsions depending on the electrical percolation threshold keeping in mind that the phase characterization provided here does not refer to the correct phase diagram due to the metastable characteristics of nanoemulsions and the conditions of the experiment. The samples were inspected after 2 and 7 days keeping in mind that samples could continue to evolve and change significantly with time.

3.2.2 The effect of temperature and surfactant concentration on the cloud point

Tween 80 ($C_{17}E_{20}$) is a polysorbitate with an ethylene oxide backbone of $w + x + y + z = 20$ providing the hydrophilic nature. The oleate moiety (C_nH_{n2n-1}, $C_{17}H_{33}$) of polysorbate 80 contains a double-bond forming a kink in the hydrocarbon chain providing the hydrophobic nature. Tween 80 has a CMC of 0.012-0.015 mM and the presence of additives may affect the temperature dependence of a nanoemulsion containing a C_mE_n surfactant. To asses this effect, the cloud point (CP) is used to determine the transition from a homogeneous micellar solution into two isotropic solution phases, one of which is rich in surfactant and the other is surfactant-poor, and is detected by an increase in the turbidity of the solution (Machado et al., 2012). Two scenarios are possible upon the use of additive. Firstly, if the CP of a C_mE_n surfactant increases, it means that the additive interacts with the surfactant aggregates, whereas a reduction in the CP suggests that the additive

is depleted from the micellar pseudo-phase (Machado et al., 2012). This behavior will be helpful in solubilizing lipophilic moieties through the generation of w/o phase. It is important to confirm the presence of this behavior during the formulation as it will have an impact on the PIT.

The CP of all solutions of $C_{17}E_{20}$ in water was determined to be 90 °C (Fig. 2). Increasing the surfactant concentration showed more turbidity without a significant change in the CP. Shinoda and Arai (1964) reported that the longer the hydrophilic chain, the higher the CP. In addition to that, a change in the volume ratio of surfactant does not have much effect on the CP compared to the temperature effect.

Figure 2

3.2.3 Effect of oil and surfactant on the PIT

The turbidity-temperature profiles of the surfactant-oil-water mixtures were measured when they were heated and then cooled in Liteszier 500 particle analyzer by measuring the %Transmission (Fig. 3). The samples demonstrated an appreciable drop in turbidity over the temperature range used in the experiment. The temperature at which turbidity first fell sharply during heating was considered as the PIT (Fig. 3). Compared to the CP temperature of 90 °C, the PIT was determined at 75 °C and confirmed that increasing hydrocarbon levels by the presence of oil decreases the CP (Shinoda and Arai, 1964). A marked decrease in turbidity was noted during cooling in the same samples and confirms the transition between w/o into o/w, passing through the bicontinuous microemulsion, which was confirmed by the conductivity measurements in the next section. Increasing surfactant concentrations had the same effect on the PIT as on the CP. This is useful to estimate the PIT from CPs of nonionic surfactants in the absence of hydrocarbons. Based on the data, the PIT emulsification process was kept at a constant temperature range between 75-85 °C to ensure the formation of bicontinuous microemulsion (Engels et al., 1995). At those high

temperatures, the interfacial tension decreases and the amount of surfactant molecules adsorbed at the o/w interface increases gradually until saturation is achieved (Yu et al., 2012). Cooling was done as part of phase inversion composition (PIC) method by the dilution of microemulsion with water to bring the temperature to 30 °C below the PIT to obtain nanoemulsions that are stable and avoid coalescence (Chuesiang et al., 2018).

Figure 3

3.2.4 The impact of water phase composition on phase inversion

It is known that microemulsions generally have low conductivity but it is significantly higher than that of pure oils such as oleic acid and coconut oil. Increasing the temperature and/or varying the molar fraction of water at constant temperature of the microemulsion, initially results in a gradual rise in its conductivity, but once a certain point is reached, there is a sudden sharp rise due to electrical percolation (Moldes et al., 2016).

The usual experiment involves adding water to an oil/surfactant mixture at constant temperature (PIT = 85 °C). A representative example of a typical conductometric experiment is reported in Fig. 4 and three regions can be identified. Upon initial addition of water (< 10% H_2O), there was an initial increase in conductivity which is attributed to hydration of the surfactant head groups and increasing their mobility (Chiappisi et al., 2016). As φw is additionally increased (~20% H_2O), the first droplets of water in oil are formed in which loratadine gets solubilized, resulting in an overall decline in κ, where its peak decline indicates the start of the electrical percolation line. After another addition of water content at ~30% H_2O, the microemulsion droplets swell until the initial concentrate of bicontinuous microemulsion is formed (Wang et al., 2008) and is represented by a sudden and sharp rises in κ, which indicates that the percolation has been threshold reached. The same transparent electrically conducting one-phase microemulsion was observed at 90 °C by

(Wadle et al., 1993). However, as soon as the phase transition to the nanoemulsion phase takes place and o/w nanoemulsions are formed, κ increases only moderately with increasing water (~70% H_2O) which was characterized as single, slightly shining blue and milky nanoemulsions. Additional dilution leads to a clearing of the nanoemulsion due to reduction in the volume fraction of the dispersed material (Heunemann et al., 2011).

The mechanism for the formation of nanoemulsion by PIC approach (Tirnaksiz et al., 2010) suggested the following events: (i) upon the first addition of water, water droplets will form in the continuous oil phase and (ii) further addition of water changes the spontaneous curvature of surfactant. The system starts as w/o microemulsion passing through bicontinuous structure, after which the water droplets merge and then decompose into smaller droplets upon further increase in the water content. From the point of view of phase inversion by temperature, raising the temperature leads to the dehydration of surfactant, triggering the formation of a w/o emulsion. Once the temperature decreases upon the addition of water, the bicontinuous microemulsion forms. Therefore, we propose that the two approaches augment each other to form a stable nanoemulsion in our experiment.

The method proposed for the production of nanoemulsion involved a preparation of microemulsion template in which a substantially insoluble drug such as loratadine is totally soluble in the dispersed or internal phase with appropriate emulsifier such as Tween 80 and external phase with limited solubilizing activity. However, microemulsion has high concentrations of surfactant, rendering it not ideal for topical application due to low kinetic stability. Therefore, the formation of nanoemulsion from a microemulsion template will be a good option.

Figure 4

Considering the influence of the compositions (i.e. surfactant; water and oil) on the appearance of bicontinuous structure, a ternary phase diagram is constructed for phase inversion feasibility domain (PIFD) at PIT (Anton et al., 2008). The domains included all compositions, which do, or do not, exhibit a peak of electrical conductivity. All the generated nanoemulsions in this study, showing droplet diameters below 100 nm exhibited conductivity. The results confirm the presence of bicontinuous structure where higher concentrations of surfactant were present as observed by Anton et al. (2008).

It was also observed that increasing surfactant concentration resulted in an increase in the nanoemulsion region (Fig. 5). All formulations prepared from phase diagrams that expanded the nanoemulsion region to an aqueous-rich apex could be diluted to a greater extent.

Figure 5

To ensure that the formation of microemulsion with small initial particle size, was relatively low below 40 nm, high surfactant content (ranging from 3-12% w/w) was used in some preparations (Pons et al., 2003). Small particle size of microemulsion may be attributed to the structure of the initial phase as the dilution involved the oil droplets that were already present without the need for the transformation from the bicontinuous structure to the closed oil structures (Pons et al., 2003). In both methods of preparation, the nanoemulsion was prepared by a two-step phase inversion that involved water dilution at the in the final stage, in a proportion of 1:5 (final water concentration was at 96-98%) to form the nanoemulsion. Well-defined phase inversion methods previously reported did not use total amount of surfactant above 10% (Tirnaksiz et al., 2010). Smaller particle size was also linked to higher water content, and thus offer better stability (Solè et al., 2012). The dilution is important for two reasons, firstly microemulsions have high concentration of surfactant

(up to 15% in our experiments) which is not favorable from the regulatory point of view (Chen et al., 2015) and secondly to ensure the formation of nanoemulsions with good kinetic stability (Wooster et al., 2008).

However, the order of mixing had no significant effect ($p > 0.05$) on the particle size, in method 1, with the particle size increasing as the surfactant concentration increased in contrast to method 2 in which the particle size decreased as the surfactant increased. In both methods, the droplet size appeared to be constant within 20% of water dilution. The findings are consistent with data reported by Solè et al. (2012) and showed the particle size is independent of the dilution of the microemulsion. The data showed that the use of phase inversion emulsification method at 80 - 95 w/w % water can result in the formation of emulsions with droplet size below 40 nm and independent of the water content as reported by Morales et al.(2003). It was suggested that the mechanism of nanoemulsion formation requires complete solubilization of the oil phase in a bicontinuous microemulsion before dilution with water (Morales et al., 2003).

The use of ultrasound in the nanoemulsions proved efficient in producing nanosystems having very small diameters with low energy consumption as it provides sufficient shear rate (Delmas et al., 2011a). It is also important to note that the production of nanoemulsions-after the microemulsion formation- requires energy input to overcome the oil/water interfacial tension which makes the ultrasound with phase inversion emulsification a feasible approach (Delmas et al., 2011b).

Table 3

3.2.5 The effect of shear

We suggested the use of Ultra-Turax homogenizer instead of simple mechanical stirring in this method because this would create a high hydrodynamic shear tool around or above the PIT in order

to extend the microemulsion or bicontinuous structure domains and to ensure all the oil phase was completely solubilized, therefore yielding a fairly monodispersed system (Roger et al., 2010). In our study, we did not obtain nanoemulsions having smaller droplets size below 100 nm when we used simple mechanical stirring compared to Roger et al. (2010) because the O/S ratio used was low (0.2-0.1). However, this can be considered as an advantage of forming a stable nanoemulsion at low surfactant concentration.

3.3 Loratadine entrapment in nanoemulsions

Loratadine entrapment was analyzed using HPLC and the EE in nanoemulsions ranged from 99.30 % to 65.02 % as shown in Table 4. For the same surfactant ratio, changing the lipid type had significant effect ($p < 0.05$) on drug entrapment. It is noteworthy that the amount of loratadine in all formulations was set at the saturated level shown in Table 1, because beyond these concentrations, nanoemulsions will break. Nanoemulsions with oleic acid showed better drug loading and it can be explained that the amount of oleic acid is enough to solubilize loratadine compared to the amount of coconut oil. It is important to note that we tried to increase the amount of oil (data not shown) to solubilize the drug but the resultant nanoemulsions were not stable.

The solubilization capacity was generally high for any water content at higher temperature. As the temperature increased the solubility of the ethoxylated surfactant decreased and which is because the mixture will be hydrophobic so that its packing at the interface will be looser, allowing more drug molecules to be integrated at the interface (Garti et al., 2006).

However, DL noticeably decreased with surfactant concentration increases and this may be attributed to the higher surface coverage of droplet (Table 3) by the surfactant that may lead to more packing (less space) of the surfactant and hindering the drug encapsulation to some extent even at higher temperature.

Table 4

3.4 Influence of oil type and surfactant concentration on the mean droplet diameter and particle size distribution

Table 5 shows particle size measurement, PDI and zeta potential of nanoemulsions using dynamic light scattering technique, which measures the fluctuations of scattered light intensity caused by particles movement. It can cover particle size ranges from a few nanometers to about 3 microns. One characteristic feature of this technique is smaller particles result in more intense light scattering compared to larger once. In general, the results showed that the mean droplet diameter remained below < 45 nm regardless of the oil used ($p > 0.05$).

Anton and Vandamme (2009) reported that nanoemulsion parameters such as particle size, polydispersity index (PDI) and droplet concentration are linked to proportion of different components of nanoemulsion.

Table 5

In terms of surfactant concentration, it was expected that increasing surfactant content would improve oil solubilization of nanoemulsion droplets. In Method 1, the particle diameter relatively increased as the surfactant concentration increased (Guttoff et al., 2015). This may be attributed to the order of mixing which involved the preheating of oil and water phases under Ultra-Turax homogenization, followed by ultrasonication and dilution with water. The use of high surfactant concentration can help the transport of nanoemulsion droplet via micelles, which may drive droplet growth by Ostwald ripening and coalescence (Rao and McClements, 2012).

In contrast, Method 2 showed the opposite behavior with increased concentration of surfactant, where particle size decreasing as the surfactant concertation increased (Guttoff et al., 2015); which may be attributed to the order of mixing which involved the preheating of oil and water phases followed by dilution with Ultra-Turax homogenization and followed by ultrasonication.

3.5 The effect of ultrasound

Ultrasound might have helped to overcome the influence of high surfactant concentration on droplet growth by reducing the contact between the nanoemulsion droplets and micelles as

suggested by Rao and McClements (2012). The application of ultrasound is known to form nanoemulsions of small particle size with narrow distribution by two mechanisms not offered by other mechanical devices-, which are (a) droplet disruption and (b) droplet coalescence. The former mechanism is governed by the type and amount of shear force applied to droplets and their resistance to deformation which is determined by the surface tension (Li and Chiang, 2012). The latter mechanism, droplet coalescence, results from the surfactant's capacity to adsorb onto the surface of newly formed droplets. This depends on the surface activity and concentration of the surfactant (Li and Chiang, 2012).

In light of the aforementioned mechanisms, Method 1 was performed by the application of ultrasound on heated undiluted emulsion during the phase inversion (w/o to bicontinuous structure) by temperature approach (step 1). At this point, the amount of shear force applied to droplets (droplet disruption) was less efficient to disrupt the droplets, as the propagation medium of ultrasonic waves is predominantly oil. As a result, the droplet coalescence mechanism will prevail and surfactant adsorption ability decreases, which triggers more coalescence even in the presence of higher Tween 80 concentrations.

On the other hand, in Method 2, the emulsion was first diluted at a temperature above the PIT and then sonicated. This allowed the system to invert from a w/o to an o/w nanoemulsion upon dilution and offering the ultrasound waves a better medium to propagate and disrupt the droplets. In the presence of high surfactant concentration and surface activity of 100% (Table 3), the nanoemulsion will give high surfactant adsorption capacity and prevent particles from coalescing.

Ultrasonic time is a significant parameter for the thermodynamic equilibrium in an o/w emulsion and influences the rate of adsorption of surfactants to the droplet surface and the size distribution of newly formed droplets. Larger droplets are formed during longer ultrasonic time (> 5 min) and which could be ascribed to the impact of emulsification over-processing, leading to the droplets coalescence (Li and Chiang, 2012).

One important advantage of our proposed method is the controlling of the system's viscosity via temperature and composition with the application of ultrasound for a short time (5 min) to form stable nanoemulsions. However, in both methods, formulations with various concentrations of surfactant, did not show significant change in the particle size ($p > 0.05$) and did not exceed 45 nm at any water content above 90% as demonstrated by Garti et al. (2016). In this study, the effective

hydrodynamic diameter of Tween 80 micelles was 10.35 ± 0.64 nm and is in agreement with the value determined by Karjiban et al. (2012) which was between 2.8-6.4 nm. The use of oleic acid and coconut oil increased the particle size to about 45 nm suggesting the oil insertion between the surfactant tails rather than forming a core within the micelles. This is in good agreement with data reported by Rao and McClements (2012).

3.6 The effect of dilution

In terms of water dilution, the particle size did not change by changing the droplet volume fraction as excess water acted only as dilution medium (Yu et al., 2012; Morales et al., 2003). It was reported that the initial droplet size is dictated by bicontinuous phase structure during the phase inversion-induced by either temperature or composition (Yu et al., 201 2; Solè et al., 2012).

The reason for rapid cooling-dilution is that extensive droplet coalescence occurs when the systems spend more time in the droplet coalescence zone during slow cooling-dilution (Saberi et al., 2015). The temperature of water for dilution was set at 25 °C because our preliminary experiments showed that dilution at 15 °C promoted gelation similar to results reported by Rao and McClements (2010). Studies have shown that stable o/w emulsions with small droplets can be obtained using the PIT method when the difference was 20-65 °C below the PIT (Shinoda and Saito, 1969). In our study, the optimum temperature (25 °C) for surfactant/oil/water system used was about 60 °C below the PIT. This will be indicative to predict optimal storage temperature (Rao and McClements, 2010).

Figs. 6a & b showed the effect of oil on the particle size distribution using oleic acid and coconut oil. Unimodal distribution of small particles of oleic acid around 50 nm was observed, which suggests that all oil phase droplets had dissolved and formed swollen micelles (Fig. 6a). In the case of coconut oil used (Fig. 6b), a multimodal distribution was noticed with a population of small particles around 15 nm and confirms the formation of nanoemulsion. In addition, a population of large particles were observed around 500 nm, which may suggest the presence of swollen micelles and undissolved nanoemulsion droplets. This is consistent with observation reported by Rao and McClements (2012) and indicates that the critical oil concentration of the drug used was almost reached (~ C_{sat}).

It is also worth mentioning that the viscosity of oils used could dictate the droplet size distribution of nanoemulsions during formation and upon storage (Wooster et al., 2008). At the PIT, the viscosities of oleic acid and coconut oil are reduced to about 5.61 and 7.55 cP from 17.7 and 28 cP at 37 °C (Noureddini et al., 1992).

Figure 6 a & b

This reduction in viscosity at PIT with the optimization of surfactant concentration can lead to the formation of small nanoemulsions (Wooster et al., 2008) and this was observed in our study, for nanoemulsions prepared from coconut oil with various surfactant concentrations.

It is also important to note that the purity of nanoemulsion components has a role on the phase behavior investigations. For example, the response to temperature of technical grade surfactants could be entirely different from that of the pure system because the partition of surfactant counterparts between water and oil is distinct from each other (Yu et al., 2012).

Small particle size has an impact on the drug permeation through stratum corneum (SC) by shortening the lag time. Choi and Maibach (2005) reported that the SC has small virtual pores in the range of 20 nm to 40 nm. Polydispersity index is a measure of distribution of the molecular mass in a given sample. PDI values > 0.7 indicates that the sample has broad range of particle size distribution, while values < 0.05 are rarely seen and cannot be considered for estimation, however, PDI < 0.3 has been considered an ideal monodispersed system. A polydispersed system is at risk of particle size growth due to Ostwald ripening in which smaller particles with high surface energy adhere to larger particles to form an energetically more stable system. The nanoemulsions had a PDI ranging from 0.19 to 0.4. This indicates that the nanoemulsions had a narrow size distribution, and suggests the monodispersity of the system which reflects positively on the system stability. In some cases, there was a slightly broad range of particle size distribution, which is a known drawback to implementing ultrasound as a tool for particle size reduction (Naseri et al., 2015). It was observed that there was a slight increase of the PDI, which might be ascribed to the weak interactions between oil droplets in agreement with previous literature data (Yu et al., 2012).

3.7 In vitro drug release studies

All formulations showed an initial burst release of loratadine which can be attributed to drug movement from the drug enriched ~~shell~~ core (Figs. 7a & b) and the drug enriched ~~shell~~ core formation can be explained by the mechanism of lipid precipitation during cooling. After hot homogenization, each droplet is a combination of lipid and drug. Cooling accelerates lipid precipitation at the core and raises the drug concentration in the outer liquid lipid and complete cooling produces ~~shell~~ core enriched with the drug. This structural model and its rapid release are suitable for dermatological formulations that are intended for increased drug permeation. It is also possible that high surfactant concentration resulted in the burst release of loratadine (Mishra et al., 2018).

Results showed a release of 54% to 83% over a period of 24 h, as shown in Figs. 7a and b. The low release profile for some of the formulations can be attributed to the low aqueous solubility of loratadine and the structural integrity of the lipid which makes the drug take longer time to diffuse out from the inner core to the outer medium.

Statistically, there were no significant effects ($p > 0.05$) on drug release because of oil phase composition, surfactant concentration and the method of preparation, except when the oil phase composition from oleic acid to coconut oil changed at constant 1:10 ratio of Tween 80, where it showed a significant effect ($p < 0.05$) on the drug release for both methods (1 and 2), which could influence the drug permeation through the skin. This might be attributed to the increased packing of Tween 80 as its concentration increases (Kogan et al., 2008) as well as the viscosity of coconut oil compared to oleic acid, which both hinder the drug release from the system.

To investigate the drug release behavior, kinetic modeling was performed to predict the rate and the mechanism of drug release. The drug release from nanoemulsions was best fitted ($R^2 = 0.993$) to zero order kinetic model as they showed highest R^2 values compared to other kinetic models (first order, Higuchi and Korsmeyer-Peppas). It means that drug release is independent of the amount of drug remaining in the formulation and this behavior was also noted by Djekica's group (2012) from microemulsion formulations.

Figure 7 a & b

3.8 Skin permeation studies

The permeation of nanoemulsions was examined using porcine skin and compared to the permeation of loratadine aqueous saturated solution. Loratadine aqueous saturated solution showed very low flux in the skin (0.09 μg/cm^2/h) while all the nanosystems showed an enhanced permeation with varying enhancement ratios. Cumulative amount of loratadine permeated after 24 h through pig skin from nanoemulsions prepared with oleic acid as oil phase showed an increase in the enhancement ratio with increasing surfactant concentration and decreased as the surfactant increased. This was observed with oleic acid nanoemulsion (OA-5), where the ER was 41.3 times, with flux equal to of 3.75 μg/cm^2/h which was significantly higher ($p < 0.05$) compared to the permeation from the aqueous saturated solution (Fig. 8a).

OA-7 and OA-10 nanoemulsions showed a decreasing ER of 11.5 and flux of 1.05 μg/cm^2/h, and 19.6 and a flux of 1.78 μg/cm^2/h respectively and the permeation was not significant between OA-7 and OA-10 ($p > 0.05$). This is consistent with the work by Yuan et al. (2010) who reported that there is a plateau surfactant concentration beyond which the drug permeation will decrease. As a result, there was only a minor effect of surfactant concentration on the mass transfer coefficients in oleic acid nanoemulsions. These formulations also had the highest EE%, which is one of the factors affecting permeation.

The same behavior was observed when coconut oil was used as an oil phase. Fig. 8b showed no significant difference between the resultant fluxes ($p > 0.05$) and this may be attributed to the insignificant difference ($p > 0.05$) among the obtained particle sizes for these formulations. CO-5 flux was 0.65 μg/cm^2/h followed by 0.58 μg/cm^2/h and 0.25 μg/cm^2/h for CO-10 and CO-7 respectively while the enhancement ratios were 7.1, 2.7, and 2.1 respectively. Changing the surfactant ratio did not show any significant enhancement in loratadine permeation ($p > 0.05$) which means the possible penetration enhancement effect of Tween 80 is not mainly responsible for the improved skin delivery neither had a significant effect on particle size. In contrast, increasing Tween 80 concentration in both oils reduced the drug permeation which might be attributed to the increased packing of surfactant as its concentration increases and in turn hinder the drug release from the system (Kogan et al., 2008).

Nanoemulsions prepared with coconut oil generally showed less permeation in comparison to those made with oleic acid. This may be due to the structure of coconut oil consisting of higher

levels of short chain saturated fatty acids such as lauric acid (makes up about 50% of the fatty acids in coconut oil). These fatty acids have insufficient lipophilic characteristics to actively permeate the stratum corneum, thus, rendering poor penetration (Viljoen et al., 2015). These sets of nanoemulsions with coconut oil of moderate permeation enhancement compared to oleic acid proved that the latter has a role in improving the loratadine permeation through the skin. Oleic acid exerts its penetration enhancing activity via a distinctive feature of *cis* double bond at C9 which bends the alkyl chain and disturbs the SC lipid bilayers (Abd et al., 2018).

Figure 8 a & b

Moreover, nanoemulsions with oleic acid showed high loading capacity (near saturation) compared with coconut oil nanoemulsions. This observation is consistent with the work done by Land et al.(2006) who reported that systems with near saturation leads to a great enhancement in mass transport. This near saturation may undergo supersaturation from microemulsions during occluded application and forms an additional driving force ~~with small nanoparticles~~ as reported by Kemken et al. (1992). It was also observed that drugs tend to become supersaturated in the microenvironment upon dilution and grow into crystals (Aserin and Garti, 2005). We suggest that this effect plays a pivotal role in enhancing the drug permeation from those nanoemulsions containing oleic acid at high surfactant concentrations (OA-7 and OA-10) and coconut oil nanoemulsions (CO-5, CO-7 and CO-10).

However, all nanoemulsions showed improved skin drug permeation *in vitro* that can be via different mechanisms and loratadine crystallization in nanoemulsions does not affect drug permeation. There are three potential mechanisms for increased delivery of loratadine from nanoemulsions as suggested by Abd et al. (2018): (i) increased solubility of the drug in the applied nanoemulsions; (ii) improved uptake of the vehicle carrying the drug into the SC; and (iii) a direct impact on the SC membrane properties, such as enhanced fluidization of the SC lipids. Additionally, permeation rates tend to be very high from supersaturated vehicles.

Loratadine is practically insoluble in water (0.0134 mg/mL) (DrugBank, 2019). The solubilization capacity of loratadine substantially increased to 45 times in the nanoemulsion formulations containing a combination of oil phase (oleic acid and coconut oil), surfactant, and aqueous phase

compared to the saturated aqueous solution. This effect was pronounced with oleic acid nanoemulsions than the one noted with coconut oil due to the high solubility of loratadine in oleic acid nanoemulsions and this increased solubility had an impact on the nanoemulsion uptake into the SC.

Another strategy to explore the enhancement mechanisms of skin permeation was to determine the J_{max}, the maximum flux of the aqueous saturated solution, as it is known that J_{max} depends only on the thermodynamic activity of the solute in the vehicle, provided the vehicle or solute does not change the membrane characteristics (Zhang et al., 2013). It is noted that the J_{max} value was low for the aqueous saturated solution of loratadine (Figs. 8a & b), however, in contrast, J_{max} values for nanoemulsions were much greater than for control. This proves that the nanoemulsions changed the SC barrier properties. It is well known that oleic acid and lauric acid (main component of coconut oil) enhance skin permeation by disrupting SC lipid (Osborne et al., 1991).

3.9 Cryogenic TEM observation of nanoemulsions

The appearance of nanoemulsions was translucent to the naked eyes as shown in Fig. 1. Cryogenic TEM was used to observe the droplet size in the nanoemulsions and the size was correlated with the data obtained from droplet size analysis using light scattering. Cryogenic TEM showed short features visible which can be described as parts of small vesicles or intact vesicles in the range of 50 nm. In addition, there were only small micelles in the range of 10-20 nm and were monodisperse (Aserin and Garti, 2005), thus confirming the hydrodynamic diameter of micelles obtained by DLS in section 3.4 as shown in Figs. 9a & b. These observations support the postulation by Rao and McClements (2012) for the presence of Regime II where the C_{sat} of the oil is reached and results in a mixture of swollen micelles and nanoemulsion droplets. Fig. 9b showed the presence of spherical micelles. The same observation was reported by Garti et al. (2004) and was attributed to the higher concentration added of guest molecule in the system which causes a more concave curvature toward the oil. In our study, the loratadine concentration was between 25-50% of the oil phase for oleic acid and coconut oil, respectively.

Figure 9

3.10 Stability of nanoemulsions at different temperatures

The stability of nanoemulsions is an important measure that dictates the shelf life of a given formulation. The stability of the optimized nanoemulsions was tested during storage at room temperature and at cold temperature for six months as shown in Table 6. For the freshly prepared systems containing oleic acid and Tween 80, there was initially a decrease in mean particle diameter from around 62 to 43 nm (1:5), 63 to 33 nm (1:7) and 50 to 31 nm (1:10) over the first three days of storage. The same behavior was observed with coconut oil nanoemulsions. This effect indicates that oil droplets have been fully solubilized within the Tween 80 micelles for an extended period as suggested by Rao and McClements (2012). The decrease in the droplet size is clearly a transient regime of Ostwald ripening as suggested by Nazarzadeh et al. (2013) and is independent of the nature of the change. The ability of Tween 80 to enhance the stability of the colloidal dispersions can also be explained to its capacity to produce repulsive steric forces between the colloidal particles owing to its comparatively large head group size. From the other point of view, we suggest the fabrication of nanoemulsions using different phase inversion approaches with short application of ultrasound promoted long-term stability.

At 25 °C, the mean droplet diameter was noticeably increased with time during storage except for CO-10. This indicates that the nanoemulsions were unstable to droplet growth at the highest storage temperature near the PIT. This can be ascribed to the fact that the rate of Ostwald ripening and/or droplet coalescence in a nanoemulsion rises in the temperature range just below the PIT (Chuesiang et al., 2018). This acceleration in coalescence might be attributed to the partial dehydration of Tween 80 head groups resulting in relatively low interfacial tension and the monolayers become highly flexible, which facilitates the fusion of oil droplets when they collide. At 4 °C, there was no significant change in mean droplet diameter throughout storage for the nanoemulsions except in CO-10.

In the case of CO-10, it showed a significant decrease in particle size over time at 25 °C from 23 to 13 nm. This suggests that higher concentrations of hydrophilic surfactant is effective in solubilizing a medium chain triglyceride such as coconut oil. The addition of lipophilic loratadine at approximately 50% of the oil phase (acts as ripening inhibitor) exerts an optimal compositional effect by reducing the oil's aqueous solubility, if added together prior to homogenization (Ryu et

al., 2018) (Chuesiang et al., 2018), however, this behavior requires further studies. The same effect was not observed with OA-10 nanoemulsion.

Table 6

Despite the rise in mean particle diameter during storage, all of the nanoemulsions appeared visibly stable to creaming throughout the 6-month storage period, due to their small droplet sizes. However, we observed that all the nanoemulsions had loratadine crystals formed within 20 days after preparation. This can be due to nanoemulsion cooling which resulted in drug supersaturation in the oil and/or aqueous phases, which would favor nucleation and crystal growth as proposed by Li et al., (2012). Varying parameters such as surfactant concentration, oil type and preparation method could not completely prevent loratadine crystal formation beyond 20 days of storage, and the same was reported by Li et al., (2012).

Nanoemulsions have excellent stability against creaming, sedimentation, flocculation and coalescence due to small droplet size compared to coarse emulsions. However, they can undergo degradation via two well-known distinctive irreversible demulsification processes: coalescence and Ostwald ripening. Coalescence occurs due to collision of droplets with each other (Wang et al., 2008). The change in droplet size with time can be described by the following equation if the instability mechanism is coalescence:

$$\frac{1}{r} = r_0^2 \left(\frac{8\pi}{3}\right) \omega t$$

where r is the average droplet radius after time t, r_0 is the droplet radius at t = 0, and ω is the frequency of rupture per unit surface of the film.

Ostwald ripening is found to be the main mechanism producing instability in nanoemulsions (Li and Chiang, 2012). Ostwald ripening occurs due to the difference in the radius between droplets, and the difference in chemical potential of the oil phase between different droplets. In the ripening process, larger droplets grow at the expense of smaller ones due to molecular diffusion through the continuous phase. The Ostwald ripening rate, ω can be obtained by LSW (Lifshitz–Slezov–Wagner) theory:

$$\omega = \frac{dr^3}{dt} = \frac{8}{9} = \frac{C(\infty)\gamma V_m D}{\rho RT}$$

where r is the average droplet size after time t, $C(\infty)$ is the bulk phase solubility (the solubility of the oil in an infinitely large droplet), γ is the interfacial tension, Vm is the molar volume of the oil, D is the diffusion coefficient of the oil in the continuous phase, ρ is the oil density, and R is the gas constant.

Fig. 10a suggests that there is no linear relationship upon plotting $1/r^2$ as a function of time and indicates that coalescence is not the basic mechanism for the nanoemulsion instability. On the other hand, there was a good linear relationship between r^3 and time as shown in Fig. 10b indicating that the main instability process was indeed the asymptotic regime of Ostwald ripening and Brownian-induced coalescence and they are valid for very diluted emulsions where drop interactions are negligible (Nazarzadeh et al., 2013). It is worth noting that the presence of multimodal distribution as shown in Fig. 6b suggests that flocculation as another mechanism of destabilization, was operative with Ostwald ripening in nanoemulsions (Nazarzadeh et al., 2013). Nevertheless, in this study, Ostwald ripening only occurred during the initial storage period. After 6 months of storage, the droplet size of nanoemulsions remained stable indicating that loratadine's ripening inhibitory function with ultrasound was very effective in slowing down the Ostwald ripening process, similar to results obtained by other investigators (Moghimi et al., 2017).

Figure 10

4. Conclusions

Stable nanoemulsions containing saturated concentration of loratadine obtained by ultrasound-assisted two-step phase inversion and cooling-stepwise dilution process, have to the best of our knowledge, been reported for the first time in the area of transdermal drug delivery. In addition, the use of a drug molecule, loratadine, to function as a ripening inhibitor is reported for the first time. The increase in preparation temperature and water volume fraction enhanced the surfactant adsorption at the o/w interface and reduced the viscous resistance of the oil phase. As a result, the droplet diameter did not exceed 50 nm after the preparation. During the emulsification method, the droplet diameter was primarily controlled by the microemulsion framework, and excess water only served as a dilution medium. Once nanoemulsions formed, the size distributions remained unchanged over the period of 6 months. The increased insolubility of the oil phase as a result of loratadine addition in the continuous phase prevented the Ostwald ripening process dramatically. The process established in this study is an attractive option for nanoemulsion as this technique leads to the production of long-term stability nanoemulsions. Nanoemulsions improved the in vitro permeation of loratadine up to 20 times compared to the aqueous saturated solution through porcine skin.

Acknowledgement

MD was supported by the German Research Foundation through the Collaborative Research Center SFB 840. Authors thank Anton Paar Middle East Technical Centre, Dubai, United Arab Emirates for their support.

References

Abd, E., Benson, H., Roberts, M., Grice, J., 2018. Minoxidil Skin Delivery from Nanoemulsion Formulations Containing Eucalyptol or Oleic Acid: Enhanced Diffusivity and Follicular Targeting. Pharmaceutics 10, 19. https://doi.org/10.3390/pharmaceutics10010019

Anton, N., Benoit, J.-P., Saulnier, P., 2008. Particular conductive behaviors of emulsion phase inverting. J. Drug Deliv. Sci. Technol. 18, 95–99. https://doi.org/10.1016/S1773-2247(08)50015-3

Anton, N., Vandamme, T.F., 2009. The universality of low-energy nano-emulsification. Int. J. Pharm. 377, 142–147. https://doi.org/10.1016/j.ijpharm.2009.05.014

Aserin, A., Garti, N., 2005. Microemulsions for Solubilization and Delivery of Nutraceuticals and Drugs, in: Benita, S. (Ed.), Microencapsulation Methods and Industrial Applications. Taylor Francis, pp. 345–428. https://doi.org/10.1201/9781420027990.ch12

Azeem, A., Rizwan, M., Ahmad, F.J., Iqbal, Z., Khar, R.K., Aqil, M., Talegaonkar, S., 2009. Nanoemulsion Components Screening and Selection: a Technical Note. AAPS PharmSciTech 10, 69–76. https://doi.org/10.1208/s12249-008-9178-x

Blanco-Prieto, M.J., Guada, M., Sebastian, V., Irusta, S., Feijoo, E., Dios-Vieitez, M. del C., 2015. Lipid nanoparticles for cyclosporine A administration: development, characterization, and in vitro evaluation of their immunosuppression activity. Int. J. Nanomedicine 6541. https://doi.org/10.2147/IJN.S90849

Chen, H., An, Y., Yan, X., McClements, D.J., Li, B., Li, Y., 2015. Designing self-nanoemulsifying delivery systems to enhance bioaccessibility of hydrophobic bioactives (nobiletin): Influence ofhydroxypropyl methylcellulose and thermal processing. Food Hydrocoll. 51, 395–404. https://doi.org/10.1016/j.foodhyd.2015.05.032

Chiappisi, L., Noirez, L., Gradzielski, M., 2016. A journey through the phase diagram of a pharmaceutically relevant microemulsion system. J. Colloid Interface Sci. 473, 52–59. https://doi.org/10.1016/j.jcis.2016.03.064

Choi, M.J., Maibach, H.I., 2005. Elastic vesicles as topical/transdermal drug delivery systems. Int. J. Cosmet. Sci. 27, 211–221. https://doi.org/10.1111/j.1467-2494.2005.00264.x

Chuesiang, P., Siripatrawan, U., Sanguandeekul, R., McLandsborough, L., Julian McClements, D., 2018. Optimization of cinnamon oil nanoemulsions using phase inversion temperature method: Impact of oil phase composition and surfactant concentration. J. Colloid Interface Sci. 514, 208–216. https://doi.org/10.1016/j.jcis.2017.11.084

Cirri, M., Maestrini, L., Maestrelli, F., Mennini, N., Mura, P., Ghelardini, C., Di Cesare Mannelli, L., 2018. Design, characterization and in vivo evaluation of nanostructured lipid carriers (NLC) as a new drug delivery system for hydrochlorothiazide oral administration in

pediatric therapy. Drug Deliv. 25, 1910–1921. https://doi.org/10.1080/10717544.2018.1529209

Delmas, T., Couffin, A.C., Bayle, P.A., Crécy, F. de, Neumann, E., Vinet, F., Bardet, M., Bibette, J., Texier, I., 2011a. Preparation and characterization of highly stable lipid nanoparticles with amorphous core of tuneable viscosity. J. Colloid Interface Sci. 360, 471–481. https://doi.org/10.1016/j.jcis.2011.04.080

Delmas, T., Piraux, H., Couffin, A.C., Texier, I., Vinet, F., Poulin, P., Cates, M.E., Bibette, J., 2011b. How to prepare and stabilize very small nanoemulsions. Langmuir 27, 1683–1692. https://doi.org/10.1021/la104221q

Djekic, L., Primorac, M., Filipic, S., Agbaba, D., 2012. Investigation of surfactant/cosurfactant synergism impact on ibuprofen solubilization capacity and drug release characteristics of nonionic microemulsions. Int. J. Pharm. 433, 25–33. https://doi.org/10.1016/j.ijpharm.2012.04.070

DrugBank, n.d. Loratadine [WWW Document]. URL https://www.drugbank.ca/drugs/DB00455 (accessed 5.17.19).

Engels, T., Förster, T., von Rybinski, W., 1995. The influence of coemulsifier type on the stability of oil-in-water emulsions. Colloids Surfaces A Physicochem. Eng. Asp. 99, 141–149. https://doi.org/10.1016/0927-7757(95)03132-W

Garti, N., Avrahami, M., Aserin, A., 2006. Improved solubilization of Celecoxib in U-type nonionic microemulsions and their structural transitions with progressive aqueous dilution. J. Colloid Interface Sci. 299, 352–365. https://doi.org/10.1016/j.jcis.2006.01.060

Garti, N., Pinthus, E., Aserin, A., Spernath, A., 2016. Improved solubilization and bioavailability of nutraceuticals in nanosized self-assembled liquid vehicles, in: Encapsulation and Controlled Release Technologies in Food Systems. John Wiley & Sons, Ltd, Chichester, UK, pp. 173–203. https://doi.org/10.1002/9781118946893.ch7

Garti, N., Shevachman, M., Shani, A., 2004. Solubilization of lycopene in jojoba oil microemulsion. JAOCS, J. Am. Oil Chem. Soc. 81, 873–877. https://doi.org/10.1007/s11746-004-0994-4

Guttoff, M., Saberi, A.H., McClements, D.J., 2015. Formation of vitamin D nanoemulsion-based delivery systems by spontaneous emulsification: Factors affecting particle size and stability. Food Chem. 171, 117–122. https://doi.org/10.1016/j.foodchem.2014.08.087

Heunemann, P., Prévost, S., Grillo, I., Marino, C.M., Meyer, J., Gradzielski, M., 2011. Formation and structure of slightly anionically charged nanoemulsions obtained by the phase inversion concentration (PIC) method. Soft Matter 7, 5697–5710. https://doi.org/10.1039/c0sm01556c

Joshi, M., Patravale, V., 2008. Nanostructured lipid carrier (NLC) based gel of celecoxib. Int. J. Pharm. 346, 124–132. https://doi.org/10.1016/j.ijpharm.2007.05.060

Karjiban, R.A., Basri, M., Rahman, M.B.A., Salleh, A.B., 2012. Structural Properties of Nonionic Tween80 Micelle in Water Elucidated by Molecular Dynamics Simulation. APCBEE Procedia 3, 287–297. https://doi.org/10.1016/j.apcbee.2012.06.084

Kemken, J., Ziegler, A., Müller, B.W., 1992. Influence of Supersaturation on the Pharmacodynamic Effect of Bupranolol After Dermal Administration Using Microemulsions as Vehicle. Pharm. Res. An Off. J. Am. Assoc. Pharm. Sci. https://doi.org/10.1023/A:1015856800653

Kogan, A., Kesselman, E., Danino, D., Aserin, A., Garti, N., 2008. Viability and permeability across Caco-2 cells of CBZ solubilized in fully dilutable microemulsions. Colloids Surfaces B Biointerfaces 66, 1–12. https://doi.org/10.1016/j.colsurfb.2008.05.006

Land, L.M., Li, P., Bummer, P.M., 2006. Mass transport properties of progesterone and estradiol in model microemulsion formulations. Pharm. Res. 23, 2482–2490. https://doi.org/10.1007/s11095-006-9014-5

Leong, T.S.H., Wooster, T.J., Kentish, S.E., Ashokkumar, M., 2009. Minimising oil droplet size using ultrasonic emulsification. Ultrason. Sonochem. 16, 721–727. https://doi.org/10.1016/j.ultsonch.2009.02.008

Li, P.H., Chiang, B.H., 2012. Process optimization and stability of d-limonene-in-water nanoemulsions prepared by ultrasonic emulsification using response surface methodology. Ultrason. Sonochem. 19, 192–197. https://doi.org/10.1016/j.ultsonch.2011.05.017

Li, Y., Zheng, J., Xiao, H., McClements, D.J., 2012. Nanoemulsion-based delivery systems for poorly water-soluble bioactive compounds: Influence of formulation parameters on polymethoxyflavone crystallization. Food Hydrocoll. 27, 517–528. https://doi.org/10.1016/j.foodhyd.2011.08.017

Lopes, L.B., 2014. Overcoming the cutaneous barrier with microemulsions. Pharmaceutics 6, 52–77. https://doi.org/10.3390/pharmaceutics6010052

Machado, A.H.E., Lundberg, D., Ribeiro, A.J., Veiga, F.J., Lindman, B., Miguel, M.G., Olsson, U., 2012. Preparation of Calcium Alginate Nanoparticles Using Water-in-Oil (W/O) Nanoemulsions. Langmuir 28, 4131–4141. https://doi.org/10.1021/la204944j

McClements, D.J., 2012. Nanoemulsions versus microemulsions: Terminology, differences, and similarities. Soft Matter 8, 1719–1729. https://doi.org/10.1039/c2sm06903b

Mehnert W, M.K., 2001. Solid lipid nanoparticles Production, characterization and applications. Adv. Drug Deliv. Rev. 47, 165–196. https://doi.org/10.1016/S0169-409X(01)00105-3

Mishra, V., Bansal, K., Verma, A., Yadav, N., Thakur, S., Sudhakar, K., Rosenholm, J., 2018. Solid Lipid Nanoparticles: Emerging Colloidal Nano Drug Delivery Systems. Pharmaceutics 10, 191. https://doi.org/10.3390/pharmaceutics10040191

Moghimi, R., Aliahmadi, A., Rafati, H., 2017. Ultrasonic nanoemulsification of food grade trans-cinnamaldehyde: 1,8-Cineol and investigation of the mechanism of antibacterial activity. Ultrason. Sonochem. 35, 415–421. https://doi.org/10.1016/j.ultsonch.2016.10.020

Moldes, A., Morales, J., Cid, A., Astray, G., Montoya, I.A., Mejuto, J.C., 2016. Electrical percolation of AOT-based microemulsions with n-alcohols. J. Mol. Liq. 215, 18–23. https://doi.org/10.1016/j.molliq.2015.12.021

Morales, D., Gutiérrez, J.M., García-Celma, M.J., Solans, Y.C., 2003. A Study of the Relation between Bicontinuous Microemulsions and Oil/Water Nano-emulsion Formation. Langmuir 19, 7196–7200. https://doi.org/10.1021/la0300737

Naseri, N., Valizadeh, H., Zakeri-Milani, P., 2015. Solid Lipid Nanoparticles and Nanostructured Lipid Carriers: Structure, Preparation and Application. Adv. Pharm. Bull. 5, 305–313. https://doi.org/10.15171/apb.2015.043

Nazarzadeh, E., Anthonypillai, T., Sajjadi, S., 2013. On the growth mechanisms of nanoemulsions. J. Colloid Interface Sci. 397, 154–162. https://doi.org/10.1016/j.jcis.2012.12.018

Noureddini, H., Teoh, B.C., Davis Clements, L., 1992. Viscosities of vegetable oils and fatty acids. J. Am. Oil Chem. Soc. 69, 1189–1191. https://doi.org/10.1007/BF02637678

Osborne, D.W., Ward, A.J.I., O'neill, K.J., 1991. Microemulsions as topical drug delivery vehicles: in-vitro transdermal studies of a model hydrophilic drug. J. Pharm. Pharmacol. 43, 451–454. https://doi.org/10.1111/j.2042-7158.1991.tb03511.x

Patel, K., Padhye, S., Nagarsenker, M., 2012. Duloxetine HCl Lipid Nanoparticles: Preparation, Characterization, and Dosage Form Design. AAPS PharmSciTech 13, 125–133. https://doi.org/10.1208/s12249-011-9727-6

Penfold, J., Thomas, R.K., Li, P.X., Petkov, J.T., Tucker, I., Webster, J.R.P., Terry, A.E., 2015. Adsorption at Air-Water and Oil-Water Interfaces and Self-Assembly in Aqueous Solution of Ethoxylated Polysorbate Nonionic Surfactants. Langmuir 31, 3003–3011. https://doi.org/10.1021/acs.langmuir.5b00151

Pons, R., Carrera, I., Caelles, J., Rouch, J., Panizza, P., 2003. Formation and properties of miniemulsions formed by microemulsions dilution. Adv. Colloid Interface Sci. 106, 129–146. https://doi.org/10.1016/S0001-8686(03)00108-8

Ramulu, G., 2011. A New Validated Liquid Chromatographic Method for the Determination of Loratadine and its Impurities. Sci. Pharm. 79, 277–291. https://doi.org/10.3797/scipharm.1012-13

Rane, S.S., Anderson, B.D., 2008. What determines drug solubility in lipid vehicles: Is it predictable? Adv. Drug Deliv. Rev. 60, 638–656. https://doi.org/10.1016/j.addr.2007.10.015

Rao, J., McClements, D.J., 2012. Lemon oil solubilization in mixed surfactant solutions: Rationalizing microemulsion & nanoemulsion formation. Food Hydrocoll. 26, 268–276. https://doi.org/10.1016/j.foodhyd.2011.06.002

Rao, J., McClements, D.J., 2010. Stabilization of phase inversion temperature nanoemulsions by surfactant displacement. J. Agric. Food Chem. 58, 7059–7066.

https://doi.org/10.1021/jf100990r

Roger, K., Cabane, B., Olsson, U., 2010. Formation of 10-100 nm size-controlled emulsions through a sub-PIT cycle. Langmuir 26, 3860–3867. https://doi.org/10.1021/la903401g

Ryu, V., McClements, D.J., Corradini, M.G., McLandsborough, L., 2018. Effect of ripening inhibitor type on formation, stability, and antimicrobial activity of thyme oil nanoemulsion. Food Chem. 245, 104–111. https://doi.org/10.1016/j.foodchem.2017.10.084

Saberi, A.H., Fang, Y., McClements, D.J., 2015. Thermal reversibility of vitamin E-enriched emulsion-based delivery systems produced using spontaneous emulsification. Food Chem. 185, 254–260. https://doi.org/10.1016/j.foodchem.2015.03.080

Shinoda, K., Arai, H., 1964. The correlation between phase inversion temperature in emulsion and cloud point in solution of nonionic emulsifier. J. Phys. Chem. 68, 3485–3490. https://doi.org/10.1021/j100794a007

Shinoda, K., Saito, H., 1969. The Stability of O/W type emulsions as functions of temperature and the HLB of emulsifiers: The emulsification by PIT-method. J. Colloid Interface Sci. 30, 258–263. https://doi.org/10.1016/S0021-9797(69)80012-3

Solè, I., Solans, C., Maestro, A., González, C., Gutiérrez, J.M., 2012. Study of nano-emulsion formation by dilution of microemulsions. J. Colloid Interface Sci. 376, 133–139. https://doi.org/10.1016/j.jcis.2012.02.063

Song, J.-H., Shin, S.-C., 2009. Development of the loratadine gel for enhanced transdermal delivery. Drug Dev. Ind. Pharm. 35, 897–903. https://doi.org/10.1080/03639040802680289

Tadros, T., Izquierdo, P., Esquena, J., Solans, C., 2004. Formation and stability of nano-emulsions. Adv. Colloid Interface Sci. 108–109, 303–318. https://doi.org/10.1016/j.cis.2003.10.023

Tavares, L., Shevchuk, I., Alfonso, M., Marcenyac, G., Valia, K., 2016. LORATADINE TRANSIDERMAL DEVICE AND METHODS. US009259397B2.

Tirnaksiz, F., Akkus, S., Celebi, N., 2010. Nanoemulsions as Drug Delivery Systems;, in: Fanun, M. (Ed.), Colloids in Drug Delivery. New York, pp. 221–244.

Venkateswarlu, V., Manjunath, K., 2004. Preparation, characterization and in vitro release kinetics of clozapine solid lipid nanoparticles. J. Control. Release 95, 627–638. https://doi.org/10.1016/j.jconrel.2004.01.005

Viljoen, J.M., Cowley, A., du Preez, J., Gerber, M., du Plessis, J., 2015. Penetration enhancing effects of selected natural oils utilized in topical dosage forms. Drug Dev. Ind. Pharm. 41, 2045–2054. https://doi.org/10.3109/03639045.2015.1047847

Wadle, A., Förster, T., von Rybinski, W., 1993. Influence of the microemulsion phase structure on the phase inversion temperature emulsification of polar oils. Colloids Surfaces A Physicochem. Eng. Asp. 76, 51–57. https://doi.org/10.1016/0927-7757(93)80060-R

Wang, L., Mutch, K.J., Eastoe, J., Heenan, R.K., Dong, J., 2008. Nanoemulsions prepared by a two-step low-energy process. Langmuir 24, 6092–6099. https://doi.org/10.1021/la800624z

Wong, H.L., Bendayan, R., Rauth, A.M., Wu, X.Y., 2004. Development of solid lipid nanoparticles containing ionically complexed chemotherapeutic drugs and chemosensitizers. J. Pharm. Sci. 93, 1993–2008. https://doi.org/10.1002/jps.20100

Wooster, T.J., Golding, M., Sanguansri, P., 2008. Impact of Oil Type on Nanoemulsion Formation and Ostwald Ripening Stability. Langmuir 24, 12758–12765. https://doi.org/10.1021/la801685v

Yu, L., Li, C., Xu, J., Hao, J., Sun, D., 2012. Highly Stable Concentrated Nanoemulsions by the Phase Inversion Composition Method at Elevated Temperature. Langmuir 28, 14547–14552. https://doi.org/10.1021/la302995a

Yuan, J.S., Yip, A., Nguyen, N., Chu, J., Wen, X.Y., Acosta, E.J., 2010. Effect of surfactant concentration on transdermal lidocaine delivery with linker microemulsions. Int. J. Pharm. 392, 274–284. https://doi.org/10.1016/j.ijpharm.2010.03.051

Zhang, Q., Li, P., Liu, D., Roberts, M.S., 2013. Effect of Vehicles on the Maximum Transepidermal Flux of Similar Size Phenolic Compounds. Pharm. Res. 30, 32–40. https://doi.org/10.1007/s11095-012-0846-x

CRediT author statement

Omar Sarheed: Conceptualization, Methodology, Supervision, Writing- original draft preparation, reviewing and editing. **Douha Shouqair:** Investigation, Writing- original draft preparation. **KVRNS Ramesh:** Supervision. **Taha Khaleel:** Investigation. **Muhammad Amin:** Investigation. **Joshua Boateng:** Investigation, Writing- reviewing and editing. **Markus Drechsler:** Investigation, writing- reviewing and editing.

Table Captions

Table 1: Amounts of lipids required to solubilize 50 mg of loratadine in lipid vs. water.

Table 2: Composition of primary microemulsion concentrates (% w/w) containing 0.3% w/w of loratadine.

Table 3: O/S ratio, droplet volume fraction and surface coverage of droplets of nanoemulsions produced by Method 1 and Method 2.

Table 4: Drug entrapment and drug loading percentages of different formulations.

Table 5: Particle size measurement, polydispersity index (PDI) and zeta potential of different formulations.

Table 6: Particle size measurements of different formulations after six-month storage.

Table 1

Lipid	Amount (mg)
Stearic acid	50
Oleic acid	100
Cetyl alcohol	150
Stearyl alcohol	150
Coconut oil	200
Carnuba wax	250

	Beeswax		250

Table 2

Formulation[a]	Oil	Tween 80	Water
OA-5	0.6	3.0	96.4
OA-7	0.6	4.2	95.2
OA-10	0.6	6.0	93.4
CO-5	1.2	6.0	92.8
CO-7	1.2	8.4	90.4
CO-10	1.2	12.0	86.8

[a] OA: Oleic acid, CO: Coconut oil and the number represent the concentration of surfactant used in the formulation

Table 3

Formulation	O/S ratio	Droplet volume fraction (φ)	Surface coverage % (Γ)[a]
OA-5 / (Method 2)	0.160	0.0072	88
OA-7 / (Method 2)	0.125	0.0096	98
OA-10 / (Method 2)	0.090	0.0132	100
CO-5 / (Method 1)	0.166	0.0144	100
CO-7 / (Method 1)	0.125	0.0192	100
CO-10 / (Method 1)	0.090	0.0264	100
CO-5 / (Method 2)	0.166	0.0144	100
CO-10 / (Method 2)	0.090	0.0264	100

[a] Surface coverage of 100% implies that water is saturated with Tween 80 with excess surfactant exists as micelles.

Table 4

Formulation	Drug entrapment (%)	Drug loading (%)
OA-5 / (Method 2)	99.21	49.61
OA-7 / (Method 2)	81.03	40.52
OA-10 / (Method 2)	86.06	43.03
CO-5 / (Method 1)	84.99	21.25
CO-7 / (Method 1)	67.30	16.82
CO-10 / (Method 1)	76.11	19.03

CO-5 / (Method 2)	65.02	16.26
CO-10 / (Method 2)	99.30	24.83

Table 5

Formulation	Hydrodynamic diameter (nm ± SD)	PDI (nm ± SD)	Zeta potential (Mv ± SD)
OA-5 / (Method 2)	43 ± 26	0.19 ± 0.0	-11 ± 6
OA-7 / (Method 2)	33 ± 3	0.26 ± 0.7	-11 ± 7
OA-10 / (Method 2)	32 ± 4	0.38 ± 6.9	-8 ± 4
CO-5 / (Method 1)	15 ± 6	0.26 ± 2.9	-12 ± 3
CO-7 / (Method 1)	16 ± 3	0.20 ± 0.0	-11 ± 4
CO-10 / (Method 1)	23 ± 3	0.70 ± 1.0	-11 ± 5
CO-5 / (Method 2)	30 ± 11	0.47 ± 1.0	-9 ± 4
CO-7 / (Method 2)	23 ± 8	0.43 ± 8.2	-12 ± 6
CO-10 / (Method 2)	16 ± 4	0.38 ± 7.4	-9 ± 4

Table 6

Formulation	Hydrodynamic diameter (nm ± SD) (25 °C)	Hydrodynamic diameter (nm ± SD) (4 °C)
OA-5 / (Method 2)	101±49	39±31
OA-7 / (Method 2)	52.±20	37±24
OA-10 / (Method 2)	51±24	30±27
CO-5 / (Method 1)	21±5	18±6
CO-7 / (Method 1)	17±4	20±2

CO-10 / (Method 1)	13±4	16±3

Figure Captions

Figure 1: Loratadine nanoemulsions prepared with different lipids

Figure 2: Variation of cloud point of Tween 80 ($C_{17}E_{20}$) of different concentrations with temperature. (●) 0.6%wt, (■) 0.84%wt and (▲) 1.2%wt of Tween 80.

Figure 3: Variation of PIT of nanoemulsions of different Tween 80 concentrations with temperature. (●) 0.6%wt, (■) 0.84%wt and (▲) 1.2%wt.

Figure 4: Electric conductivity measurements as a function of water concentration (Tween 80 + H_2O) at 85 °C.

Figure 5: Phase inversion feasibility domains (PIFD) diagram

Figure 6: Particle size distribution of (a) OA-7 and (b) CO-5.

Figure 7: (a) Loratadine release profile for nanoemulsions prepared using oleic acid and different Tween 80 ratios: OA-5/ (Method 2) (♦), OA-7/ (Method 2) (■) and OA-10/ (Method 2) (▲). Mean ± SD (n = 3).

Figure 7: (b) Loratadine release profile for nanoemulsions prepared using oleic acid and different Tween 80 ratios: CO-5/ (Method 1) (♦), CO-7/ (Method 1) (■), CO-10/ (Method 1) (▲) and CO-10/ (Method 2) (×). Mean ± SD (n = 3).

Figure 8: (a) Skin permeation of loratadine nanoemulsions in comparison to saturated solution prepared using oleic acid and different Tween 80 ratios: OA-5/ (Method 2) (♦), OA-7/ (Method 2) (■), OA-10/ (Method 2) (▲) and saturated solution (×). Mean ± SD (n ≥ 3).

Figure 8: (b) Skin permeation of loratadine nanoemulsions in comparison to saturated solution prepared using coconut oil and different Tween 80 ratios: CO-5/ (Method 1) (♦), CO-7/ (Method 1) (■), CO-10/ (Method 1) (▲) and saturated solution (×). Mean ± SD (n ≥ 3).

Figure 9: Cryogenic-transmission electron micrograph (Cryo-TEM) of nanoemulsions

Figure 10: Storage stability of nanoemulsions at 25 °C. (a) $1/r^2$ as a function of time (a) and r^3 as a function of time (b) for oleic acid nanoemulsions.

Figure 1

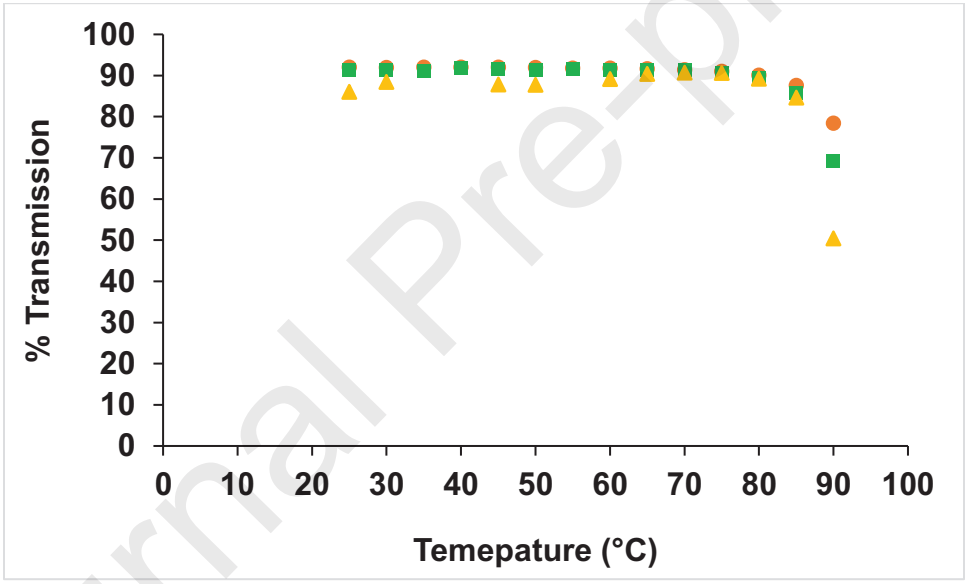

Figure 2

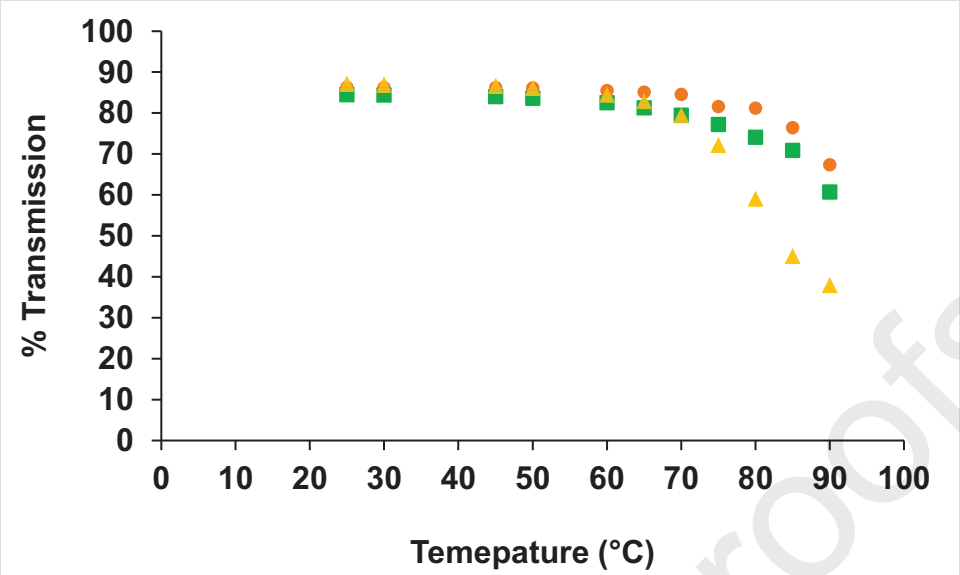

Figure 3

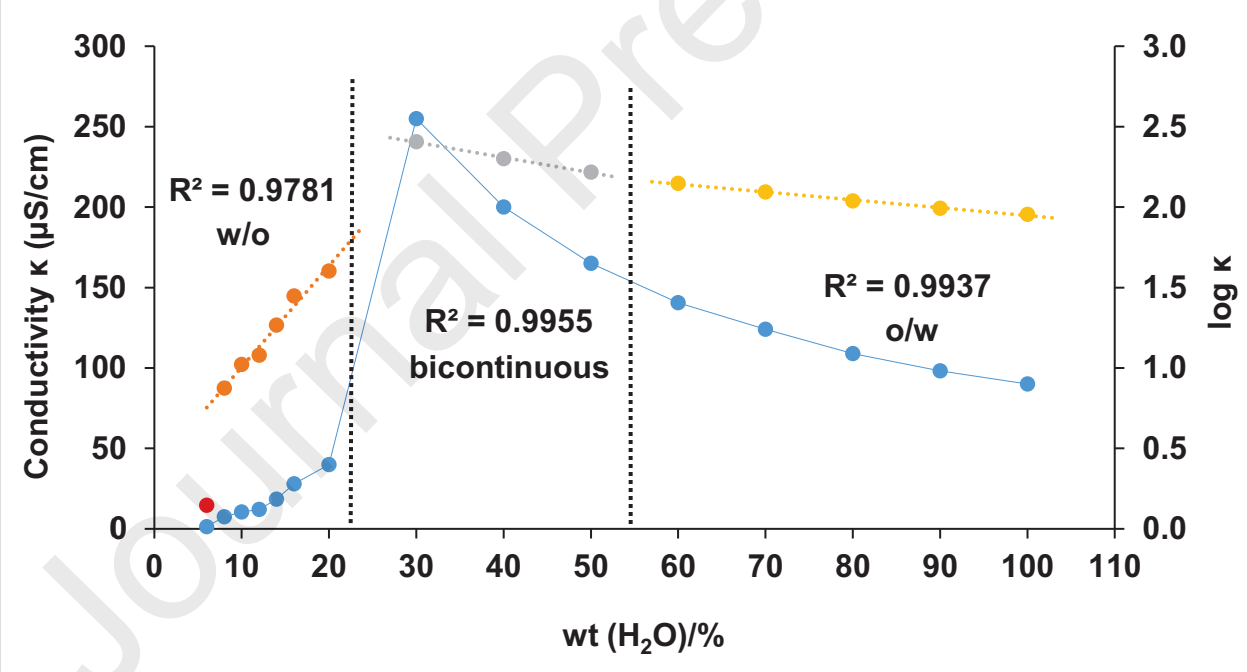

Figure 4

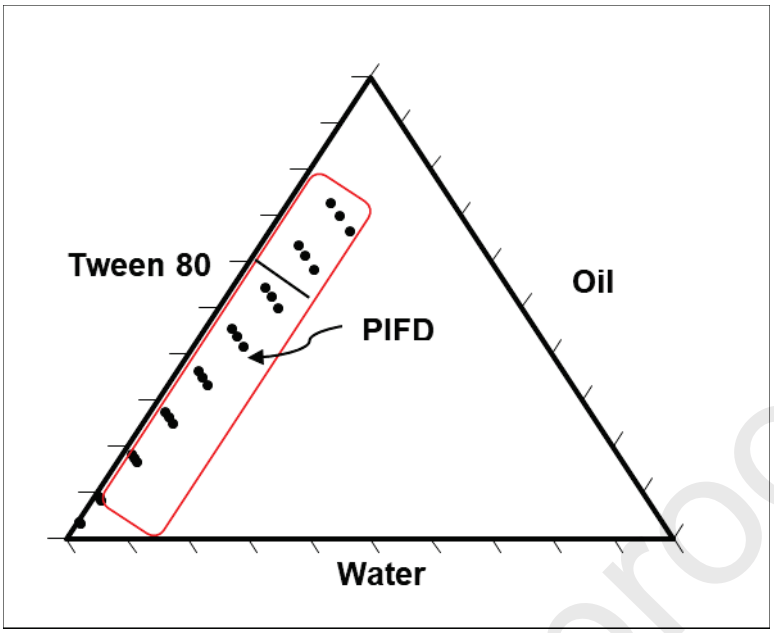

Figure 5

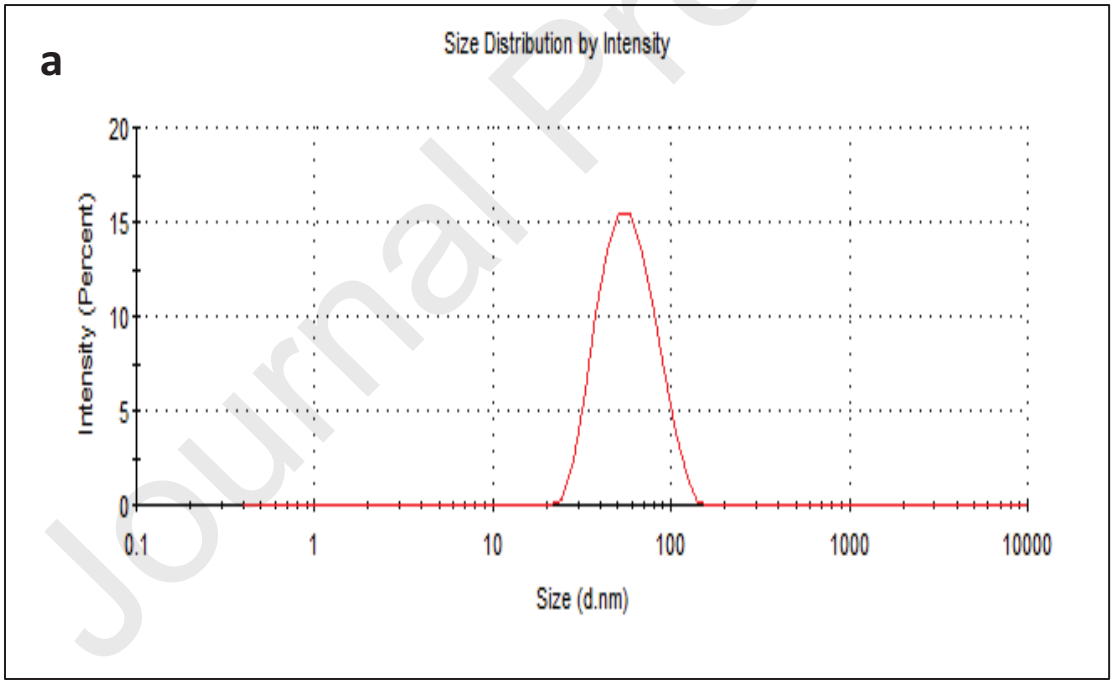

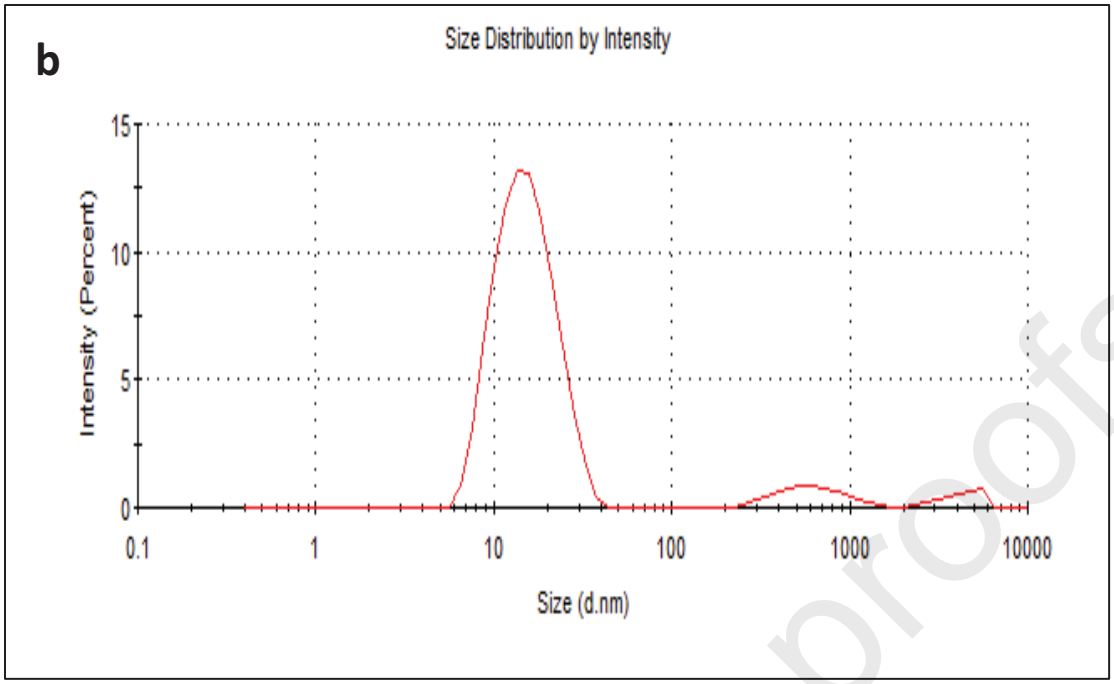

Figure 6

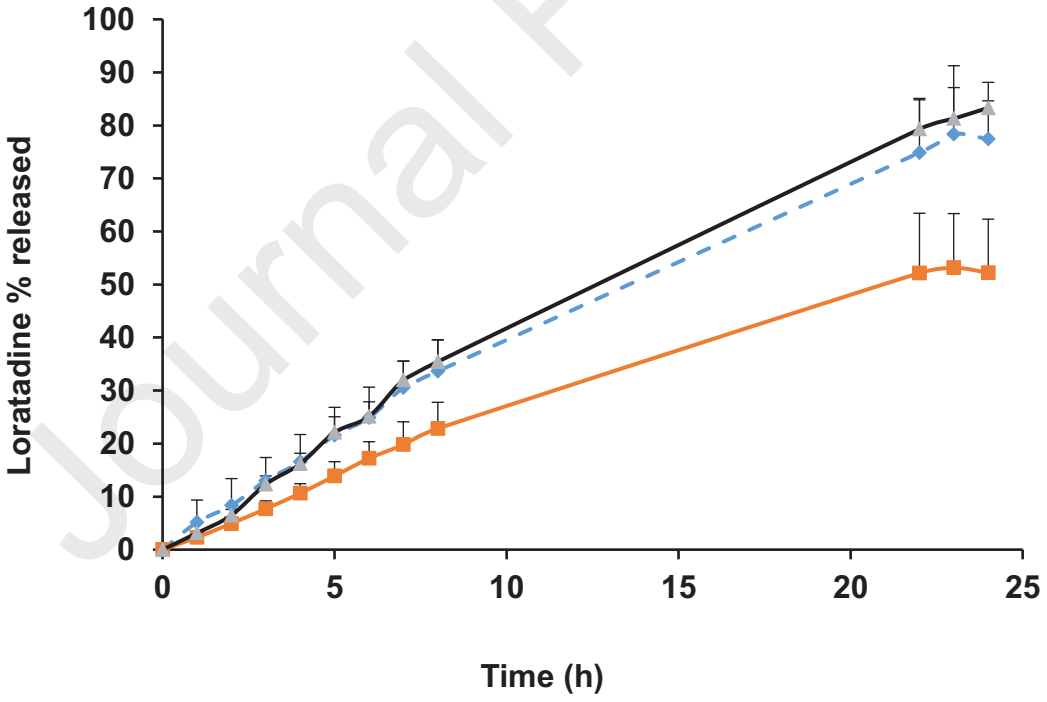

Figure 7 (a)

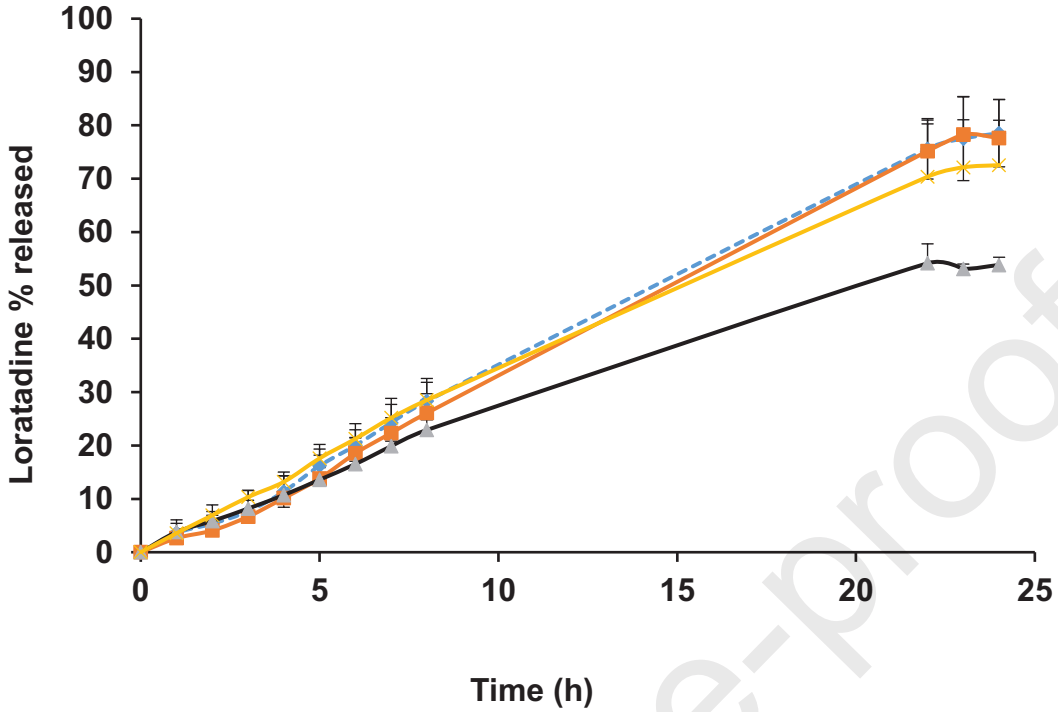

Figure 7 (b)

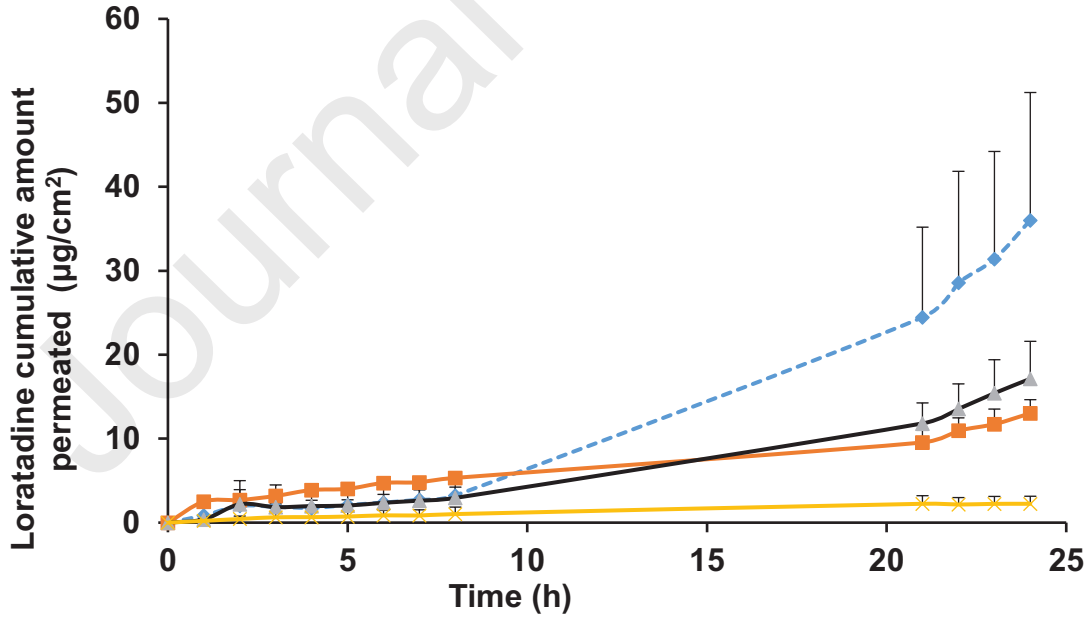

Figure 8 (a)

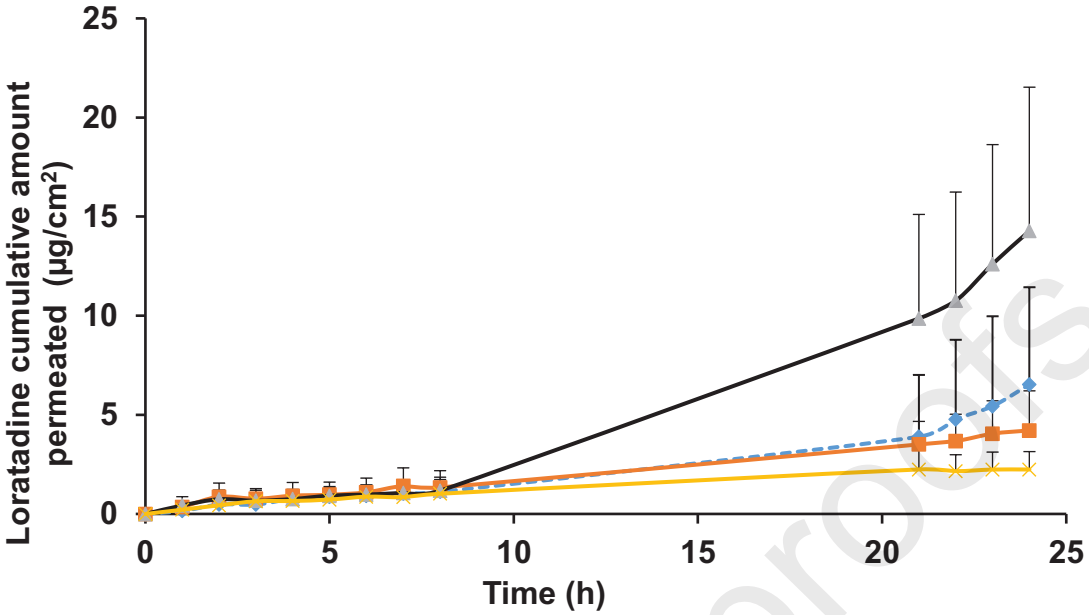

Figure 8 (b)

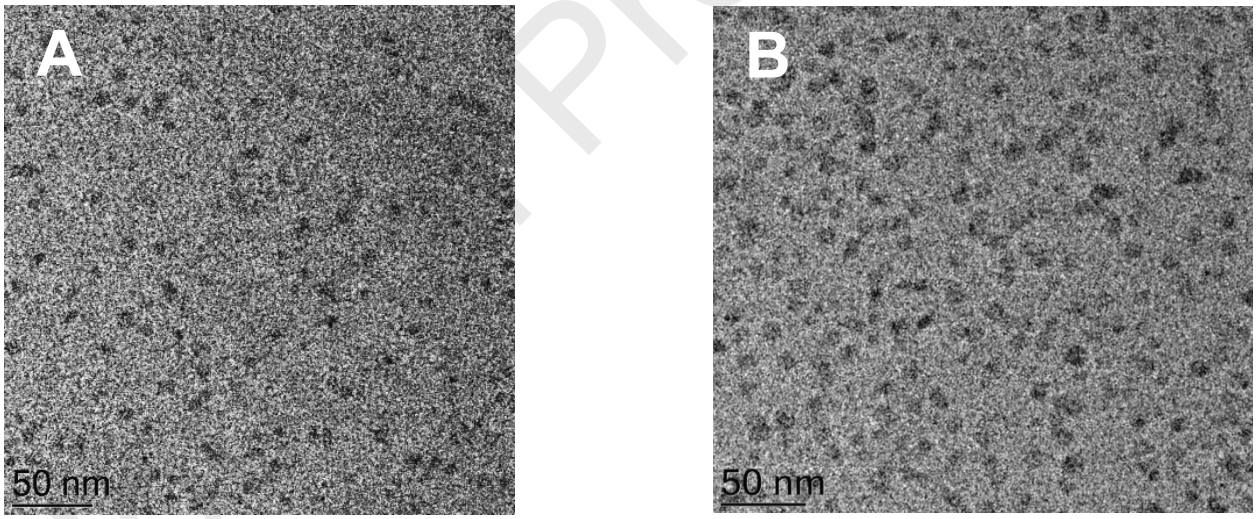

Figure 9

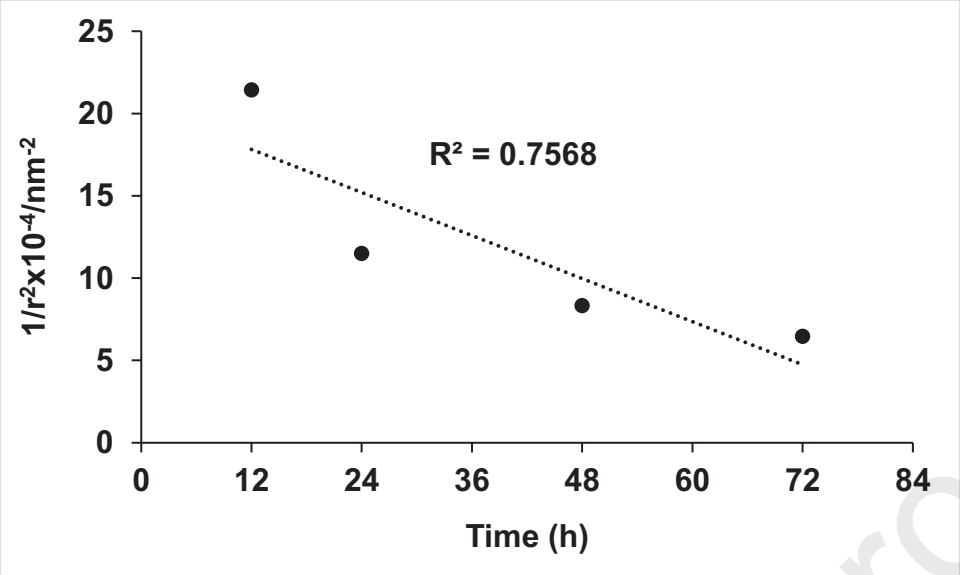

Figure 10 (a)

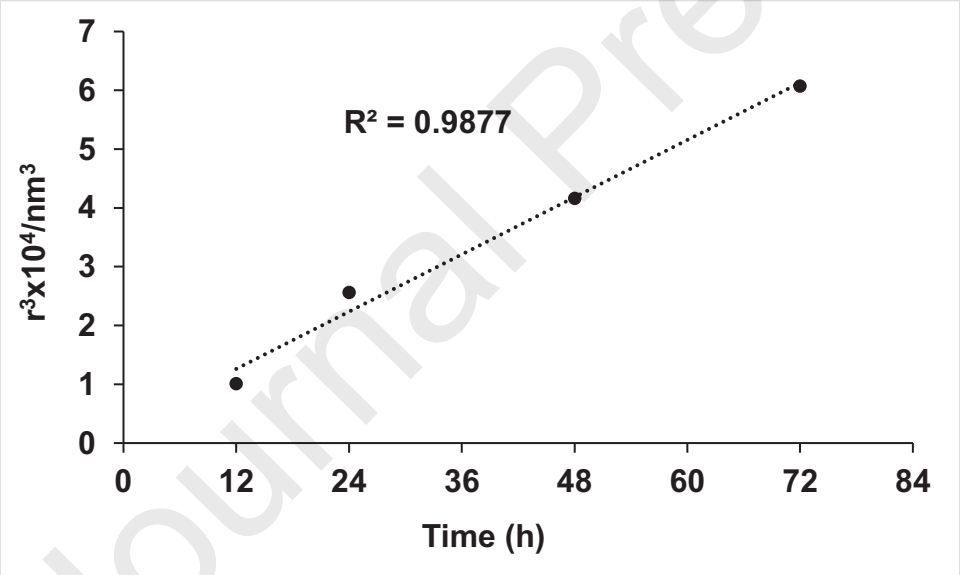

Figure 10 (b)

Declaration of interests

☒ The authors declare that they have no known competing financial interests or personal relationships that could have appeared to influence the work reported in this paper.

☐The authors declare the following financial interests/personal relationships which may be considered as potential competing interests: